12-2018

Stereotypic Repetitive Hand Flapping Movement Detector Children with Autism

Subodh Ashok Bansode
Western Michigan University

STEREOTYPIC REPETITIVE HAND FLAPPING MOVEMENT DETECTOR CHILDREN WITH AUTISM

by

Subodh Ashok Bansode

A thesis submitted to the Graduate College
in partial fulfillment of the requirements
for the Degree of Master of Science in Engineering
Electrical and Computer Engineering
Western Michigan University
December 2018

Thesis Committee:

Ikhlas Abdel Qader, Ph.D., Chair
Janos L. Grantner, Ph.D.
Michelle Suarez, Ph.D.

ACKNOWLEDGMENTS

There are many people to whom I owe a debt of thanks for their support over the last 2 years. First, I would like to express my gratitude, appreciation, and thanks to my advisor Dr. Ikhlas Abdel Qader for her support, guidance, and encouragement in completion of this thesis. She always found adequate time to oversee my studies and share her knowledge and expertise with me. She stood by not only as a supervisor but also as a mother. I would also like to express my sincere appreciation to my committee member Dr. Janos Grantner for his support and time in the preparation of this work. Moreover, I would like to thank Prof. Michelle Suarez for her support as my committee member.

I would like to express special thanks to my family for their invaluable support and guidance throughout my life. A special feeling of gratitude is directed towards my loving parents, Prajavati Bansode and Nitesh Bansode, whose words of encouragement and push for tenacity ring in my ears. My sister and brother-in-law have never left my side and are very special.

Above all, I owe my deepest gratitude and special thanks to my beloved, incredibly wonderful wife, Kiran Bansode, and my beautiful and precious daughter, Trisha Bansode. Thank you for your love, support, patience, and numerous sacrifices throughout my academic program. I love both of you more than I can say. This thesis and the pursuit of my goals would not have been possible without you.

Subodh Ashok Bansode

STEREOTYPIC REPETITIVE HAND FLAPPING MOVEMENT DETECTOR CHILDREN WITH AUTISM

Subodh Ashok Bansode, M.S.E.

Western Michigan University, 2018

The prevalence of Autism Spectrum Disorder (ASD) has increased at a significant rate in recent years, especially in developed nations such as the United States, Japan, and South Korea. Extensive research is being carried out to study the behavioral characteristics of the disease. Children affected with autism tend to exhibit a spectrum of symptoms depending on the severity of the disease. These behaviors are primarily repetitive, self-stimulatory, and stereotypic behaviors such as hand flapping (i.e., repeatedly shaking their hands), body rocking (i.e., swaying their body back and forth), drumming, walking around in a confined space, and walking with shortened steps on toes, etc. Some children with a high severity of autism exhibit abrupt and uncontrollable motions that may interrupt normal activity and be socially awkward. These behaviours may not cause immediate harm, but may hamper the learning abilities of children slowly and eventually. They may also lead to self-injurious behaviors and critical damage when harm is repeatedly inflicted in one location.

Parents who are concerned about the behavioral characteristics of autism often seek immediate treatment. They also seek the help of caregivers to look after their children. Correcting these restricted and repetitive behaviors at an early age helps children overcome them slowly. Although extensive research is being carried out in studying and categorizing the behavioral characteristics of the disease, there has not been a single technological device available in the market for aiding the autistic kids.

In this research project, a simple reminder system is proposed using wearable sensors to automatically detect significant hand flapping movements. The reminder system consists of a speaker encoded with the voice of mother, father, or any other custom designed voice. An algorithm was designed to trigger the audio device when the child showed significant hand flapping activity (i.e., hand flapping more than 10 times) within a given time frame. The time frame and the hand flapping count can be customized per severity of the child's symptoms. The device was successfully tested in the laboratory by simulating the hand flapping movement shown by the child. It is hoped that this system provides a valuable service to parents and the child by alerting the child to autistic movements, preventing the habit from turning into self-injurious behavior, and taking away the burden from parents and caregivers.

TABLE OF CONTENTS

Table of Contents—Continued

CHAPTER

Table of Contents—Continued

CHAPTER

Table of Contents—Continued

LIST OF TABLES

LIST OF FIGURES

List of Figures—Continued

INITIAL SUMMARY

Autism is classified as a neurodevelopment disorder with a spectrum of symptoms often referred to as Autism Spectrum Disorder (ASD) (Centers for Disease Control and Prevention, 2018). It is estimated that 1 in 68 children have been identified with the disease. However, autism has been increasing at an alarming rate since 2000 (i.e., 1 in 150 rate in 2000, to 1 in 88 rate in 2008, to 1 in 68 in 2012, to 1 in 45 by the end of 2015) (Centers for Disease Control and Prevention, 2018). According to MIT research scientist and author Stephane Seneff, it is predicted that 1 of out of 2 kids in the United States will be diagnosed with autism by 2025, which became quite controversial (Autism Society, 2015). The total estimated costs per year for children with ASD were between $11.5 billion and $60.9 billion in 2011. Figure 1 shows the spectrum of autism symptoms. Repetitive behavior includes hand flapping and body rocking.

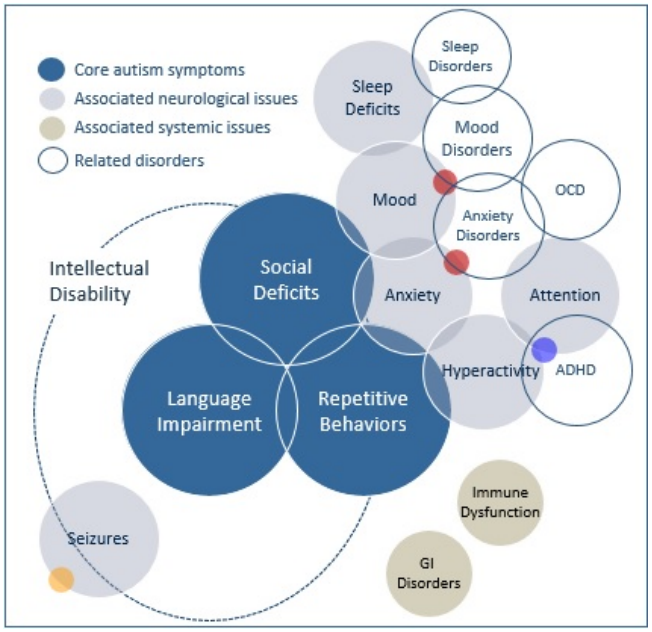

Figure 1. Basic symptoms of ASD (https://www.autismspeaks.org/what-autism/symptoms; Min & Tewfik, 2010).

Even though autism is a life-long condition, intervention and therapy can help children and adults by reducing symptoms through behavioral modification over time. It is

recommended that intervention methods are initiated as soon as possible to ensure the greatest benefits of therapy as soon as possible and throughout life (Min & Tewfik, 2010). Children and adults with ASD are susceptible to what the National Autism Association classifies as meltdowns (Autism Society, 2015). According to the organization, "A meltdown is an intense response to overwhelming situations. It happens when someone becomes completely overwhelmed by their current situation and temporarily loses behavioral control." Anticipating a meltdown can be helpful in keeping children from causing harm to themselves. In fact, strategies such as distraction including listening to music and massaging can aid in preventing a meltdown, and therefore, are considered beneficial therapies.

CHAPTER I

INTRODUCTION

Autism is a complex and varied developmental disorder that leads to deficiencies in communication and social interaction. It is usually referred to as Autism Spectrum Disorder (ASD), indicating that it exhibits a variety or spectrum of symptoms depending on the severity of the disease, the environmental surroundings, and the impact of genetic characteristics on the child. The CDC's (Centers for Disease Control and Prevention) Autism and Developmental Disabilities Monitoring (ADDM) network estimates that about 1 in 68 children have been identified with the disease. The prevalence of autism is increasing at an alarming rate since 2000 (i.e., 1 in 150 rate in 2000, to 1 in 88 rate in 2008, to 1 in 68 in 2012, to 1 in 45 by the end of 2015) (Centers for Disease Control and Prevention, 2018). MIT research scientist and author, Stephane Seneff, predicted that 1 of out of 2 kids in the United States will be diagnosed with autism by 2025, which became quite controversial (Autism Society, 2015). The total estimated costs per year for children with ASD were between $11.5 billion and $60.9 billion in 2011. These significant figures and statistics show the importance of research in ASD.

Extensive research is ongoing and focused on identifying the causes of autism. Researchers have concluded that there is no known single cause for the disease, but it is accepted that it is resultant from abnormalities in brain structure. On observing the pattern of autism related disabilities, researchers conclude that the disease has a genetic basis; that is, a cluster of unstable genes may interfere with brain development, resulting in autism. It is also observed during brain scans that there are significant differences in the shape and structure of the brain in children with autism compared to in neurotypical children. Accordingly, researchers are investigating various theories exploring the links among heredity, genetics, and medical problems. Environmental surroundings also have a significant effect on the

severity of the disease. Other problems during pregnancy or delivery, as well as environmental factors such as viral infections, metabolic imbalances, and exposure to chemicals are also being investigated (Autism Society, 2015).

Statement of the Problem

The developmental disorder of autism affects social development and the ability to communicate. They exhibit a spectrum of self-stimulatory, repetitive, stereotypic behaviors including vocal stutters and sudden and violent bouts of vigorous activity. Some of the common stereotypic behaviors seen in children affected with autism are arm flapping (i.e., repeatedly shaking hands), body rocking (i.e., repeatedly swaying their body back and forth), and drumming, etc. Some children show abrupt and uncontrollable motions and depart from their normal activity. These behaviors can be disruptive and socially awkward depending on the severity of the disease. These symptoms are not universal to all the children affected with autism, but differ from individual to individual. Sometimes, they may also differ in a single individual over the course of time.

The stereotypic behaviors may not cause immediate harm, but may hamper the learning abilities of children eventually. They may also lead to self-injurious behavior and critical damage when repeated harm is done to one location. These behaviors are stimulating, socially awkward, and may also set them apart from others. Parents are often concerned about these behaviors and seek immediate treatment to correct the behaviors. They also seek the help of caregivers to look after their children. Correcting these behaviors at an early age helps children in overcoming them slowly. Parents and caregivers are advised to look for those behaviors and correct them whenever possible to alleviate the worsening of these situations. Research also suggests that the early intervention and correction can help in improving the behaviors of their children.

As seen from the above symptoms, a computer technology that would identify and remind one of the parties (i.e., parents or children) about the stereotypic, repetitive motion can greatly reduce the efforts of parents and caregivers. In this research project, concentrated attention is given to the hand flapping movement, which is one of the major symptoms exhibited by autistic children. The device identifies when there is significant hand flap activity; that is, flapping continuously more than user defined times in a span of defined acceleration. The flap count and the time span is customizable, per the severity of the symptoms exhibited by the child. When the significant hand flap is detected, the pre-recorded father's or mother's voice can be played, which acts as a reminder and may be used as pacifying sound for the child. In a way, it acts as an emotion controller for the child.

Review of the Literature

A significant research has been devoted extensively in the field of autism in recent times. The popular areas of research in the field falls into one of the below mentioned categories:

1. Analysis of emotional state based on EEG signal
2. Stereotypic movement detection

As the focus of this research is mainly on stereotypic movement detection, less information is gathered in this literature review concerning the emotional detection procedure using the EEG signal acquisition; however, preliminary explorations have been made, if in case it helps in further research.

Analysis of Emotional State Based on EEG Signal

Electroencephalography (EEG), a popular electrophysiological method to capture the electrical activity of the brain, can be used for the emotional state analysis of autistic subjects. The EEG signal shows electrical voltage fluctuations in the brain. Researchers are increasingly utilizing the powerful capabilities of the EEG signal to study brain activity and

the associated emotions (Sprague & Newell, 1996). Some of these papers and the procedures followed are described below.

Sensory responses of autism via EEG for sensory profile. In their study, Sprague and Newell (1996) aimed to investigate the brain signal of autism children through EEG associated to physical tasks. The acquisition of brain signals was acquainted using the EEG Neurofax 9200 and the electrodes were positioned as per the International System Placement Standards (Sprague & Newell, 1996). The obtained signals were pre-processed and were analyzed using the Discrete Wave Transform (DWT) technique. The EEG signals were classified into delta, theta, alpha, beta, and gamma waves depending on the frequency range. The associated emotional states were estimated as per the Table 1 given below (Sprague & Newell, 1996).

Table 1

EEG Signals and Associated Emotional States (Sprague & Newell, 1996)

Type	**Frequency (Hz)**	**Behavior**
Delta	0.5 to 4	Deep sleep
Theta	5 to 8	Consciousness toward drowsiness
Alpha	9 to 13	Relaxing without focus and attention
Beta	14 to 30	Active thinking, full attention
Gamma	31 to 100	Finger movement

The Short Time Fourier Transform (STFT) was used to analyze the spectral content in the EEG signal, as the signal is highly non-Gaussian, non-stationary, and non-linear in nature. The sliding window technique was applied for N samples using the Fast Fourier Transform (FFT). Then, the Discrete Wavelet Transform (DWT) was applied with the associated cut-off frequencies for their feature extraction in their respective spectral components. The mean,

standard deviation, and approximate entropy were calculated to determine the emotional state of the subject (Sprague & Newell, 1996). The flow chart showing the procedure is shown in Figure 2.

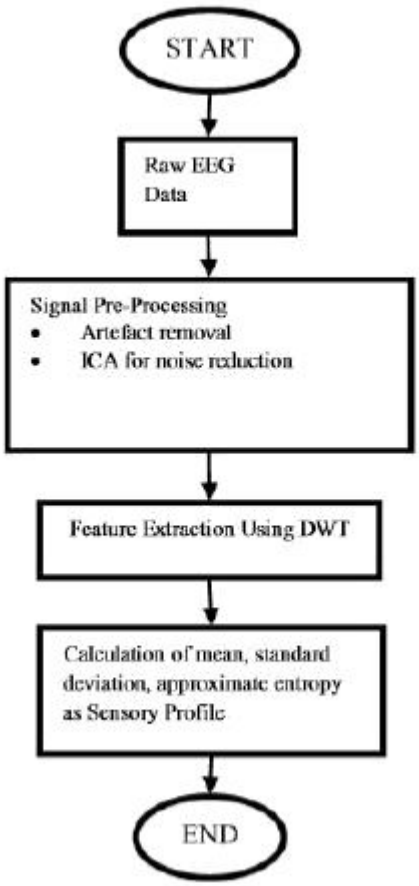

Figure 2. Flow chart of sensory profile via EEG (Sprague & Newell, 1996).

Implementation procedure and data analysis. The raw EEG data was taken from the electrodes placed at various locations on the head and processed to split the signal into its spectral components. The pre-processing of the signal starts with artifact removal and noise reduction using ICA (Sprague & Newell, 1996). Then, feature extraction was executed using DWT for the selected points of electrode. The artifact was rejected through the user interface 'MATLAB' and the noises were cleaned using the ICA method through EEGLAB. Once the artifact was removed by ICA, the signal was passed through system of filter banks of DWT. This levels down the signal to a range of frequency bands of alpha, beta, gamma, delta, and

theta, and the features were extracted. Then the mean, standard deviation and approximate entropy were calculated to obtain the emotional state of the subject as the sensory profile (Sprague & Newell, 1996).

Literature Study of Stereotypic Movement Detection

A good amount of research is being done on recognizing the stereotypic movements of the autistic child. Most of the research is mainly concentrated on just identifying the class of stereotypic movement data. These papers categorize the data obtained from various accelerometer sensor modules into specific movements such as hand flapping, body rocking, swinging, etc. The research in these papers has been confined to laboratory studies, and has not been taken beyond to help autistic kids in real time. This research has, however, provided a solid foundation to help upcoming researchers in understanding the real problem of the prevailing disease of ASD (Min & Tewfik, 2010).

Automatic characterization and detection of behavioral patterns using LPC of accelerometer sensor data. Min and Tewfik (2010) disucssed the automatic characterization and detection of these stereotypic movement behavioral patterns using the linear predictive coding (LPC) of the accelerometer data. Accelerometer based wearable sensors placed at various locations of the body were used to record the events. A PC was used to export the readings of the sensor system in real time, and time domain pattern matching with linear predictive coding was used to categorize the detected movements. A microphone and video recording tagged with real time events was simultaneously used for ground truth analysis. A new algorithm was also developed to update the dictionary based on template matching and LPC. A detection accuracy of 80% was achieved using this model. The dictionary generation and the dictionary update are obtained per the procedure is shown below in Figure 3. The classification results for flapping, rocking, punching and hitting are shown in Table 2 below.

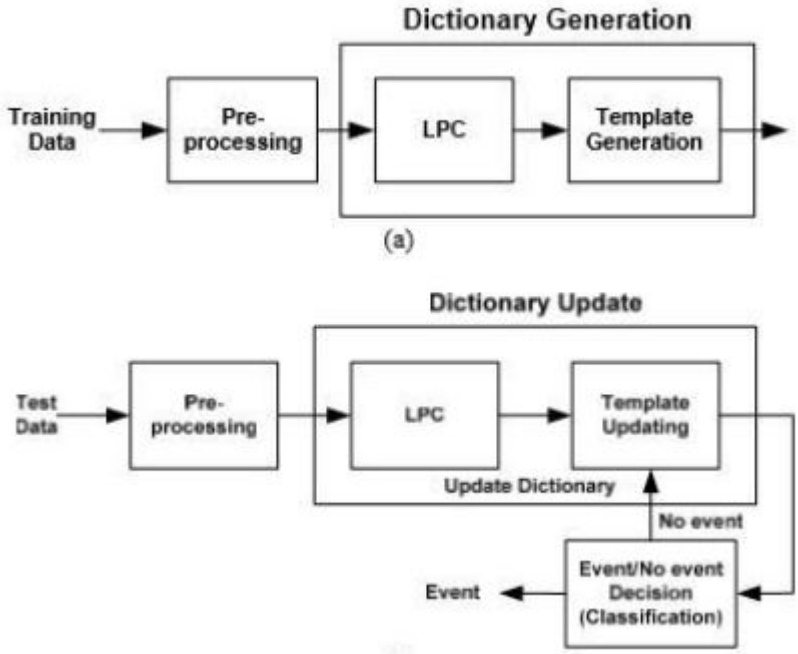

Figure 3. Training algorithm using LPC (Min & Tewfik, 2010).

Table 2

Classification Results for Behavioral Patterns (Min & Tewfik, 2010)

Classification results for flapping (F) and rocking (R)				
	Prec.(F)	Recall(F)	Prec.(R)	Recall(R)
Subject 1	87%	94%	90%	95%
Subject 2	82%	89%	93%	96%
Subject 3	85%	95%	NA	NA
Subject 4	83%	96%	NA	NA
Classification results for punching (P) and hitting (H)				
	Prec.(P)	Recall(P)	Prec.(H)	Recall(H)
Subject 1	NA	NA	NA	NA
Subject 2	NA	NA	NA	NA
Subject 3	92%	96%	NA	NA
Subject 4	NA	NA	88%	95%

Recognizing stereotypical motor movements in the classroom: A case study. An effort was presented in Min and Tewfik (2010) for recognizing stereotypical motor movements in the laboratory and classroom settings. The aim of this paper is to explore the

possibility of real time recognition of stereotypical motor movements using mobile wireless accelerometer sensors rather than traditional measuring methods such as paper-and-pencil rating scales, direct observation, and video-based methods (Sprague & Newell, 1996), all of which have limitations. The data was collected from six different participants aged between 12 and 20 years who wore sensors in laboratory and classroom settings. The study included repeated observations of body rocking and hand flapping or simultaneous body rocking and hand flapping. The wireless accelerometer sensors were placed simultaneously on the left and right wrists and on the torso to detect hand flapping and the body rocking motion. A 3-axis +/- 2g motion data at 60Hz was transmitted by three sensors and synchronized by the receiver, plugged into a standard computer. Simultaneously, a video camera was also used to for tagging the real-time data with accelerometer data. The data was collected in 10 to 30 minute sessions per week per participant for over a period of 12 months. The start time, end time, and type of stereotypical movement (i.e., hand flapping, body rocking, flap-rock) were coded in real time using custom annotation software.

In other work, Witten and Frank (2002) employed a decision tree classifier algorithm to effectively recognize a variety of physical activities. Five time and frequency domain features were computed for each acceleration data stream. They are: (1) The distances between means of the axes of each accelerometer to capture sensor orientation for posture; (2) Variance to capture the variability in different directions; (3) Correlation coefficients to capture the simultaneous motion in each axis direction; (4) Entropy to capture the type of stereotypical movement; and (5) FFT peaks and frequencies to capture differentiation between different intensities of the stereotypical movements. These features were computed for a window of data, assembled into a vector, and used as input to the C4.5 classifier in the WEKA toolkit (Witten & Frank, 2002) . The analysis and the accuracy rate of annotations of stereotypic movements varied from person to person depending on the type and duration of

stereotypic movement. The authors of the paper observed that the performance of classifiers trained on real-time annotations was slightly better than the classifiers trained using offline annotations with stereotypical motor movements of long durations (7 seconds or more). From the data collected from six children, they achieved a detection accuracy of 88.6%. They also suggested that the temporal filtering techniques on data would further improve the detection accuracy. The performance results of various participants in the classroom and laboratory settings are shown in the table below.

Table 3

Performance Results of Various Participants (Witten & Frank, 2002)

Participant ID	Train Classroom, Test Lab	Train Lab, Test Classroom
6	64.9%	64.8%
7	90.8%	86.8%
8	90.7%	91.9%
9	91.8%	83.9%
10	75.0%	73.4%
11	75.8%	87.7%
Mean	83.7%	81.4%

Recognizing Mimicked Autistic Self–Stimulatory Behaviors Using HMMs

Another similar effort was presented in research conducted by Westeyn, Vadas, Bian, Starner, and Abowd (2005), wherein the authors designed a monitoring system for children with autism. The primary concentration of the research was recognizing mimicked autistic self-stimulatory behaviors using hidden Markov models (HMM). The model was implemented with three of the small 3-axis wireless-blue tooth accelerometer sensor modules that can be embedded in child's shoes, belt, wrist watch, or clothing. The position of the sensors varied from individual to individual depending on the symptoms and behaviors

exhibited by the child. The wireless sensor data from the module 'ADXL202JE' was sampled at 100Hz by a PIC microcontroller and was sent to a dedicated personal server for further operation. The acceleration data was generated by mimicking autistic stimming behaviors. Those stimming behaviors were categorized as seven different profiles. They are: (1) drumming, (2) hand flapping, (3) hand striking, (4) pacing, (5) rocking, (6) spinning, and (7) toe walking. The hidden Markov models (HMM) were constructed for these behaviors and were trained and tested using the Georgia Gesture Toolkit. With these models, the authors accurately identified the exact boundaries of behaviors and were able to obtain detection accuracy of 68.57% (Westeyn et al., 2005).

Research Goal and Proposed Technique

The goal of this study focuses on the development of a prototype sensing system and a response synthetic stimulation system that will incorporate input from physical behavior and from user input. The system will be able to communicate both ways using a mobile phone. A feasibility study will be conducted using real clinical set-up. Feedback from the real-time testing will be used to enhance system performance. There is an array of possible realization for the proposed system in terms of sensing a behavior and responding in a sensation therapy. The final product will be a choice of the user or his caregivers and based on their needs.

Smart Bracelet

The proposed design consists of three main modules as follows:

- Module 1: Composed of a wearable wrist band for detecting specific behavior from child with autism such as hand flapping.
- Module 2: Composed of a screen and configuration module designed for the caregiver and or parent. This could also be realized through a smart phone.

- Module 3: A response module to active the system's response to the positive detection of behavior. Response selected can be composed of signal sensation such as simple vibrations with or without recorded audio messages or music through headphones.

As recordings will include uncertain behavior, all data (sensor values) will be stored in database using the cloud for diagnostic purpose. When the system senses threshold value through flapping hands, the system will automatically store data in the cloud. Data can be streamed continuously for 30 days. This data will be accelerometer data in terms of hand motion, body temperature, and heart rate.

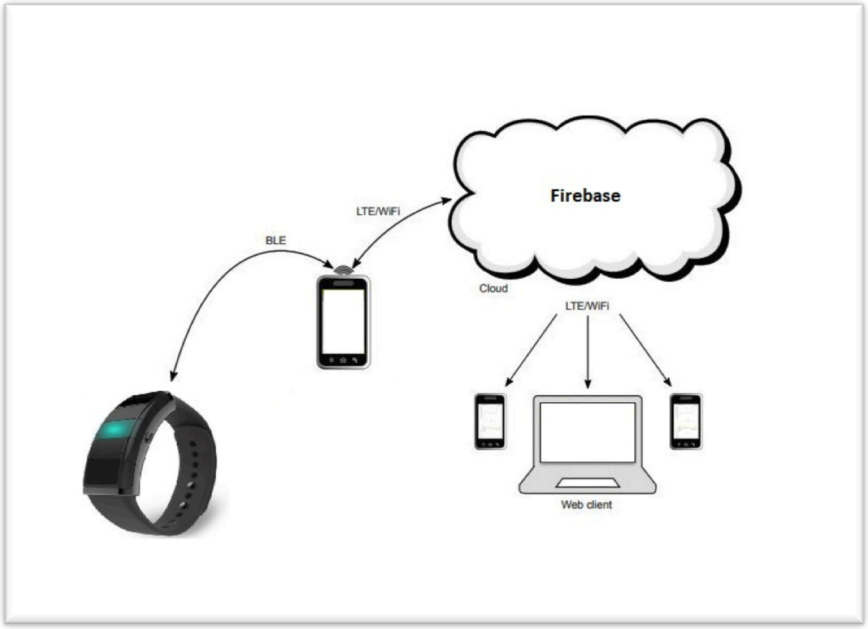

Figure 4. System overview diagram.

Related Work

A number of recent studies using an accelerometer sensor feature as sensing input to machine learning classifiers show promising results for automatically detecting stereotypical movements in individuals with ASD. However, replicating these results across different types of accelerometers and their position on the body still remains a challenge. Research has explored automated monitoring of SMM based either on webcams or accelerometers. In a series of publications, Gonçalves, Rodrigues, Costa, and Soares (2012) created methods

based on the Kinect webcam sensor from Microsoft. Their approach shows promising results, with the authors restricted themselves to detecting only one type of SMM, namely hand flapping. In addition, the Kinect sensor is limited to monitoring within a confined space and requires users to be in close proximity to the sensor (Gonçalves et al., 2012). Alternative approaches to the Kinect are based on the use of wearable 3-axis accelerometers. Although the primary aim of previously published accelerometer-based studies is to detect hand flapping in individuals with ASD, some studies have been carried out with healthy volunteers mimicking SMM, and therefore do not necessarily generalize to the ASD population (Min, Tewfik, Kim, & Menard, 2009). .

To date, there have been two different approaches to automatically detecting SMM in ASD using accelerometer data. One approach is to use a single accelerometer to detect one type of SMM, such as hand flapping when a sensor is worn on the wrist (Westeyn et al., 2005). The second approach is to use multiple accelerometers to detect multiple SMM, such as hand flapping from sensors worn on the wrist, and body rocking with a sensor worn on the torso (Albinali, Goodwin, & Intille, 2009). Other studies have done the same, but included a detection class where hand flapping and body rocking occur simultaneously in time (Maxim Integrated, 2016a,b).

While more sensors appear to improve recognition accuracy in these studies, one practical drawback is that many individuals with ASD have sensory sensitivities that might make them less able or willing to tolerate wearing multiple devices. To accommodate for different sensory profiles in the ASD population, it would be ideal to limit the number of sensors to a minimum, while still optimizing accurate multiple class SMM detection.

Thesis Outline

This thesis is structured in five chapters, including this introduction. These chapters consist of the following:

Chapter I provides a definition of autism (ASD) and proposed techniques that can used to detect hand flapping in child with autism. It also provides a review of related work researchers have done on this topic.

Chapter II consists of a description of the techniques used for detecting hand flapping, along with detection algorithm and sensors mechanism and describes all prototype designs of smart bracelet (Wise Hand), along with system validation and analysis.

Chapter III shows hardware simulation and detection algorithm results. It also highlights future possible techniques for detection algorithm.

Chapter IV concludes the thesis work with a discussion of future scopes of research.

CHAPTER II

HAND FLAPPING DETECTION USING AN ACCELEROMETER TECHNIQUE

The essential part of the system proposed for this study was an accelerometer, as it was used to detect hand flapping frequency with acceleration in autistic kids. After careful consideration and research, a basic accelerometer was selected.

An accelerometer is a device that measures *acceleration,* which is the rate of change of the velocity of an object. It is measured in meters per second squared (m/s^2) or in G-forces (g), where g = 9.8 m/s^2 (this does vary slightly with elevation and will be a different value on different planets due to variations in gravitational pull). Figure 5 presents a diagram of a three-dimensional accelerometer and three-dimensional gyroscope sensors.

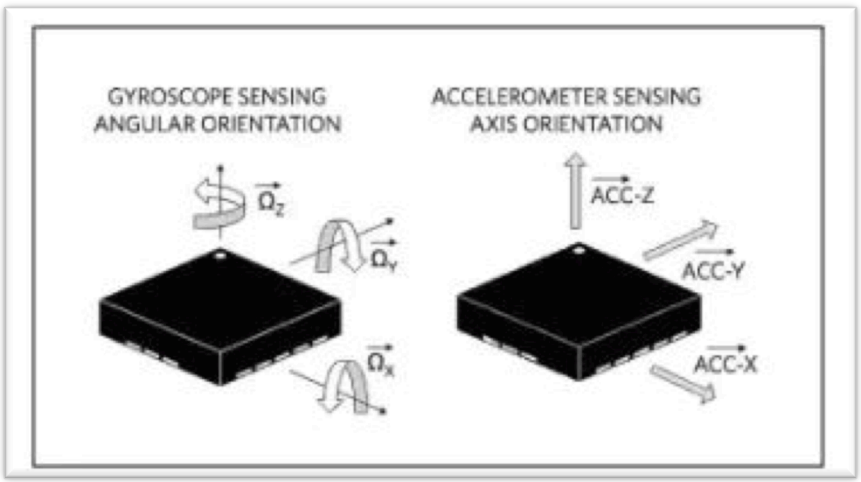

Figure 5. Three-dimensional (3D) accelerometer and 3D gyroscope sensors. Retrieved from https://www.nti-audio.com/en/support/know-how/fast-fourier-Transform-fft.

Accelerometers can measure acceleration on one, two, or three axes. Three-axis units are becoming more common as the cost of development for them decreases. Generally, accelerometers contain capacitive plates internally. Some of these are fixed, while others are attached to miniscule springs that move internally as acceleration forces act upon the sensor. As these plates move in relation to each other, the capacitance between them changes. From these changes in capacitance, the acceleration can be determined (see Figures 6 and 7).

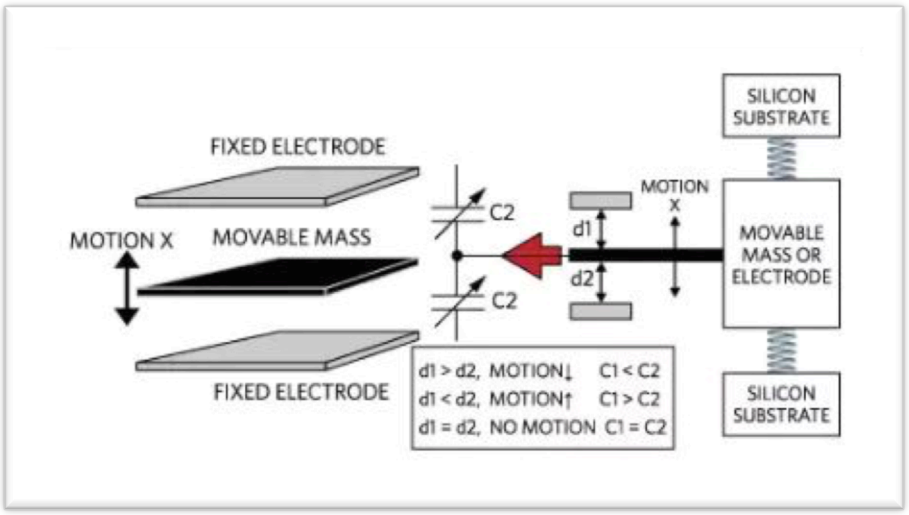

Figure 6. Accelerometer mechanism. Retrieved from https://www.nti-audio.com/en/support/know-how/fast-fourier-Transform-fft.

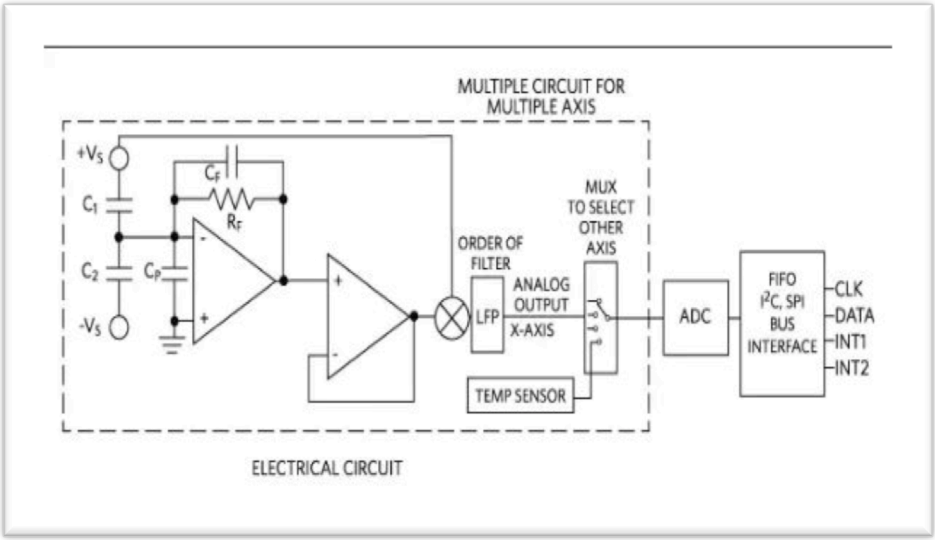

Figure 7. In a sample implementation, C1 and C2 form a voltage divider between two opposing power supplies and the output is digitized. Retrieved from https://www.nti-audio.com/en/support/know-how/fast-fourier-Transform-fft.

What is an accelerometer measure? Acceleration is how fast something is speeding up or slowing down. Acceleration is displayed either in units of meters per second squared (m/s^2), or G-force (g), which is about $9.8 m/s^2$ (the exact value depends on your elevation and the mass of the planet the object is on).

Approached Techniques for Hand Flap Detection

Recognition of the hand flap movement is challenging when compared to body rocking or swaying. The challenge is the need to identify and separate the stereotypic movement from other routine activities. For instance, when a child is trying to drink juice, the subject exhibits to and fro motion of the hand. In that case, the accelerometer and the gyroscope read the values as the motion, but it should not be considered as a stereotypic motion. Considering the issue, the concept of time span is included while writing the algorithm.

Manual and Semi-Automatic

In the manual technique (time domain), acceleration is basically being observed,and the sum of acceleration of three directions during flapping motion is set as threshold value. The time period between two hand flapping motions is also set after observation, along with flap count threshold. Whenever this threshold is met in the system, outputs get trigger (motor, alert message to parent and sensors data logged in cloud). In the semi-automatic technique (Frequency Domain), the FFT (fast Fourier transform) technique is being used to detect hand flapping frequency with a defined coefficient.

FFT Mechanism

The Fast Fourier Transform is very versatile mechanism used in signal systems. Basically, these techniques classify and separate all frequencies present in one signal. Each signal has its own identity in terms of amplitude and phase (see Figure 8). The following image in Figure 8 describes more clearly about the Fast Fourier transformation more clearly. The signal in red color is input or raw acceleration data (Time domain) and signal in blue color output applying FFT to raw signal, which separates all frequency contents.

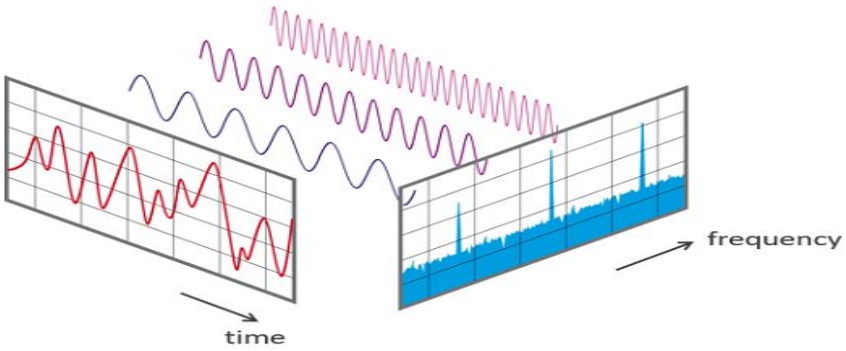

Figure 8. View of a signal in the time and frequency domain.

FFT means transformation from the time domain to the frequency domain, which is defined as

$$S(\omega) = \int_{-\infty}^{\infty} s(t) e^{-j2\pi f t}\, dt$$

Where, S(t) is signal in time domain and S(w) in frequency domain.

$$e^{-j2\pi f} = \cos 2\pi f + i \sin 2\pi f, \qquad where, i = \sqrt{-1}$$

Flow Chart

The flow charts below describes the system proposed for this study in greater depth. Figure 9 shows the processes by which movements are detected. Figure 10 shows a flow chart for automatic detection.

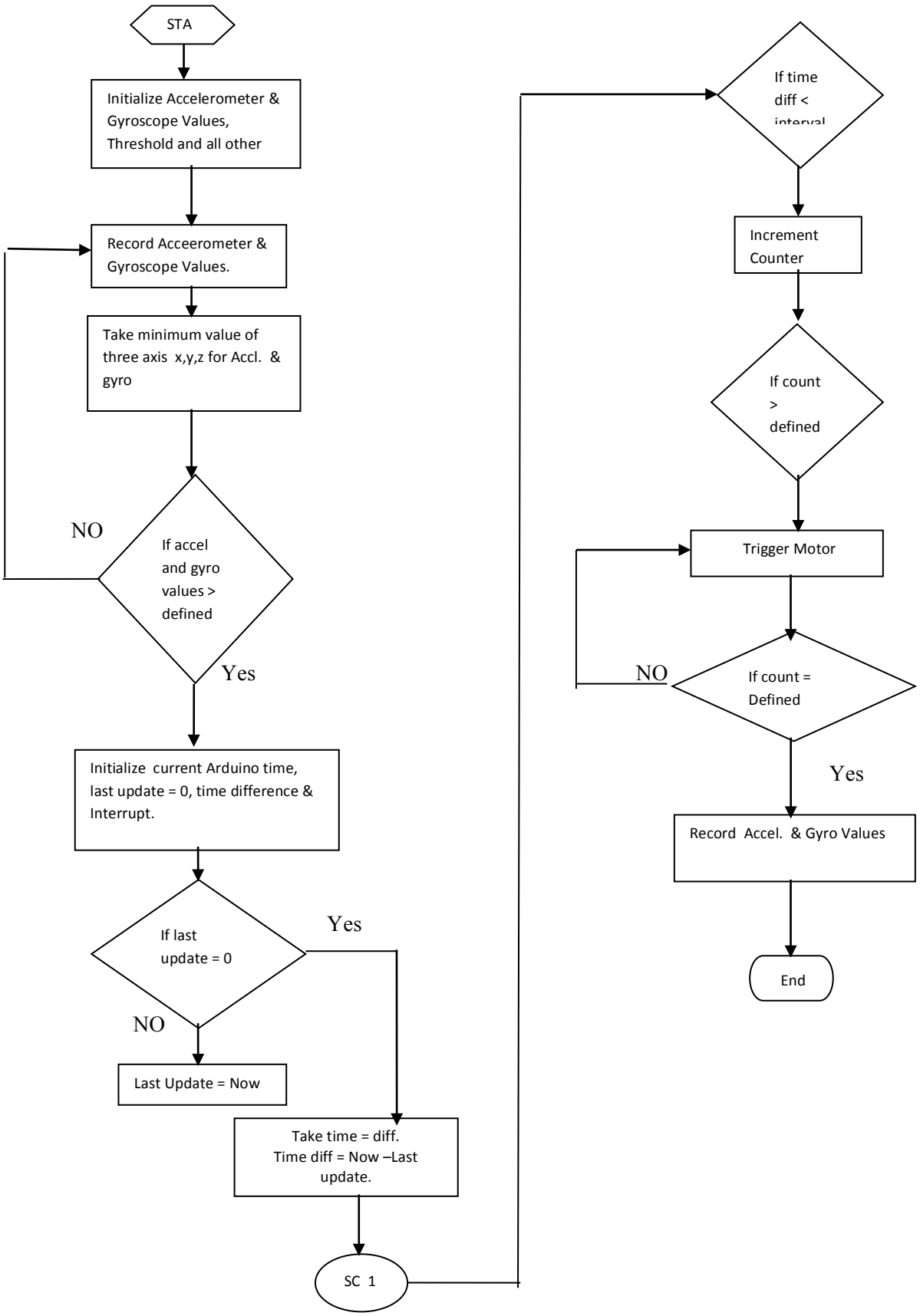

Figure 9. Flow chart of proposed system.

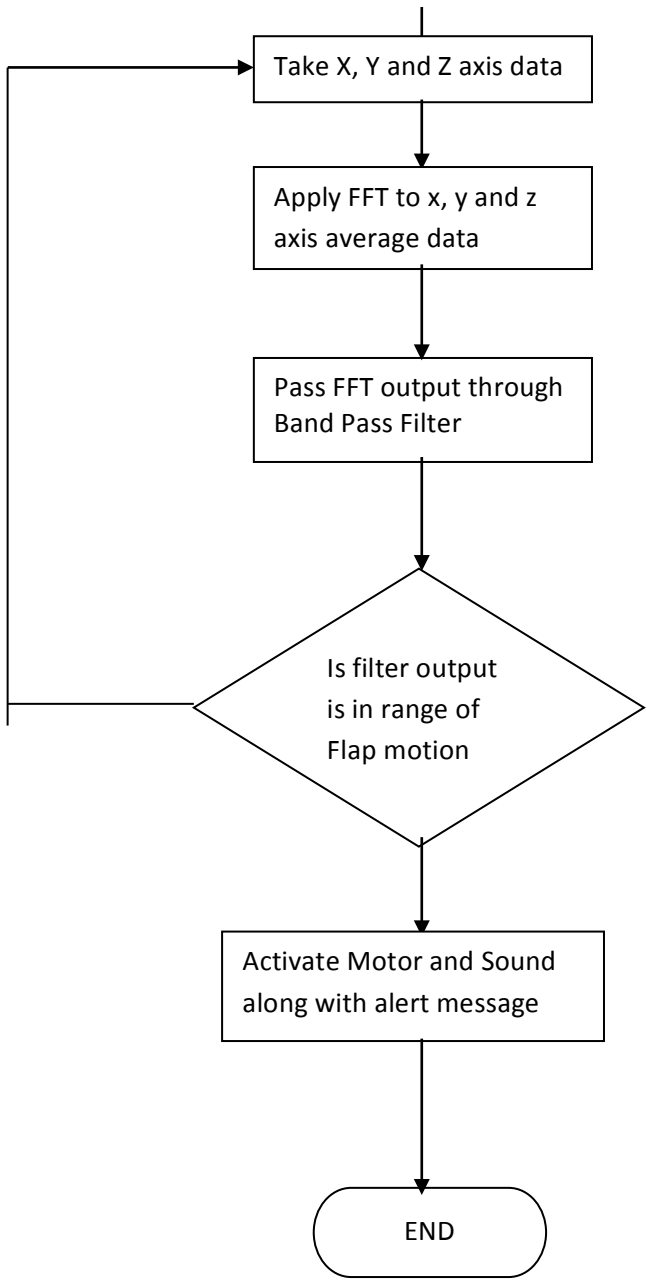

Figure 10. Flow chart for automatic detection.

Wise Hand-I Design Approached (Manual Technique)

Wise Hand-I design consists of three main modules. Module 1 is composed of a wearable wristband for detecting specific behavior from child with autism such as hand flapping (Figure 11). This system would be an essential part of this technique, as it senses all uncertain behaviors of child who has autism (i.e., flapping) using sensors (i.e., accelerometer and temperature). It should be configured through Module 2 because every child with autism can have different movements of hand flapping; based on the movement, the caretaker or parent can configure the wristband (Module1).

Module 1 is integrated with a microcontroller (Atmega), sensors (accelerometer, temperature), RTC, OLED display, and 3.7v Battery. The purpose of RTC and OLED is to make the band multipurpose, showing time and date other than sensing parameters. Even this display can attract the child to wearing it for a long time. RF24L01 is a wireless communication module, and works on a 2.4 GHz band.

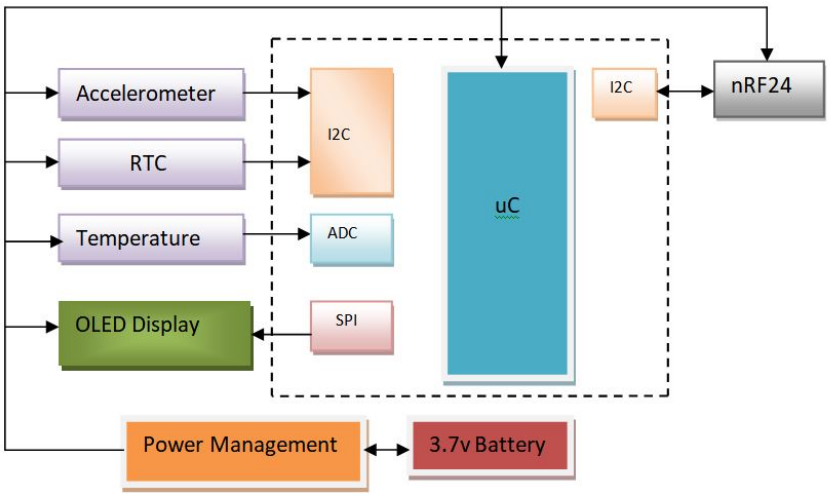

Figure 11. Module1 block diagram.

Module 2 is composed of a screen and configuration module designed for the caregiver and/or parent (Figure 12). It may also be realized through a smart phone. Basically, this system is designed for caretakers and parents. The purpose of this system is to configure

Module 1 and monitor all activity of certain or uncertain behavior (i.e., hand flapping) of child. This module is designed in such a way that it can access all sensor data any time on request; however, it also logs the sensor data when flapping takes place, which can help to future analysis purpose. The SD memory card is integrated for data storing. The Nokia 5110 display is embedded in this module with keypad for better user interface. This module also operates on 3.7v battery.

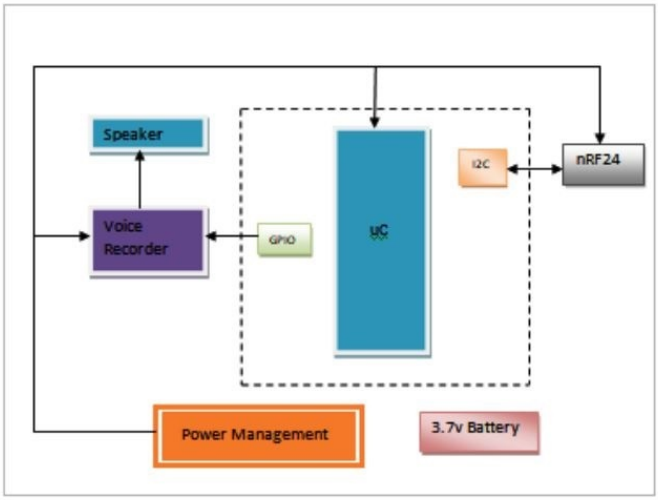

Figure 12. Module 2 block diagram.

Module 3 is a response module to activate the system's response to the positive detection of behavior (Figure 13). The response selected can be composed of signal sensation such as simple vibrations with or without recorded audio messages, or music through headphone. This module works as an alert trigger system to make the child behave normal by playing the sound of his or her parents or caregivers (in the future, there will be vibrators motors as well). This module receives a command from Module 1 (as it detects hand flapping). Once Module 3 receives a command from Module 1, it triggers the voice recorder circuit for playing of the voice. This system is integrated with a microcontroller, an ISD voice processor, a speaker, and RF24L01. All three modules are communicating in one common

wireless network using RF24L01. Each module has its separate significant function as described below.

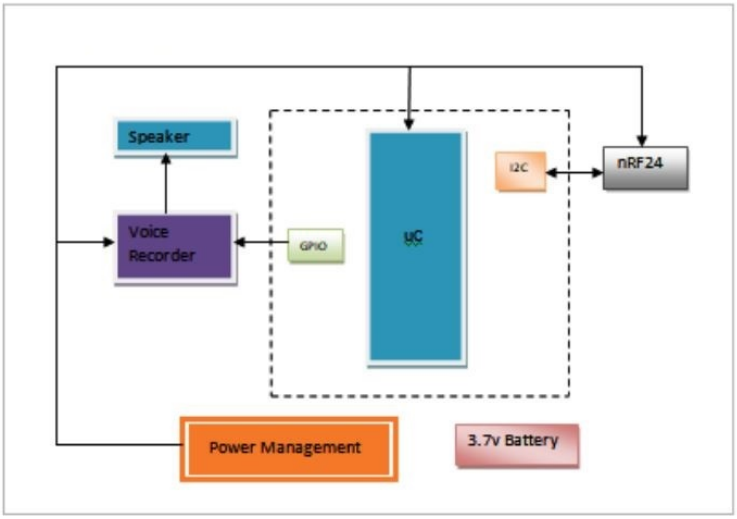

Figure 13. Module 3 block diagram.

Hardware Design of Wise Hand-I

The Atmega 328 Microcontroller was selected as for the first microcontroller design, as it is an 8-bit controller with 32 Kbytes ROM and 4 bytes of RAM. For the clock 16MHz was utilized (Microchip, 2016). These specifications were sufficient to control the accelerometer, the heart sensor, and temperature, along with wireless communication. Below is the designed schematic for the microcontroller (Figure 14).

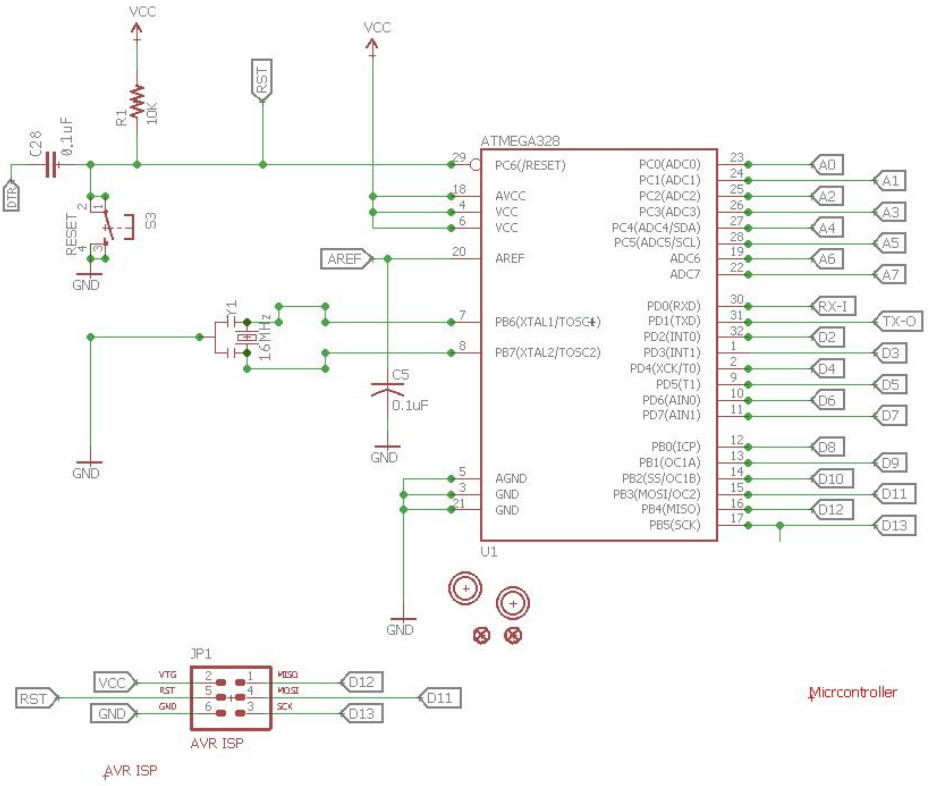

Figure 14. Atmega 328 circuit diagram.

Specifications of the Atmega 328 (Microchip, 2016)

- Program Memory Type: Flash
- Program Memory Size (KB): 32
- CPU Speed (MIPS/DMIPS): 20
- SRAM Bytes: 2,048
- Digital Communication Peripherals: 1-UART, 2-SPI, 1-I2C
- Capture/Compare/PWM Peripherals: 1 Input Capture, 1 CCP, 6PWM
- Timers: 2 x 8-bit, 1 x 16-bit
- Temperature Range (C): -40 to 85
- Operating Voltage Range (V): 1.8 to 5.5
- Sensors circuit design:
- Accelerometer Sensor:

The MPU-6050 devices combine a 3-axis gyroscope and a 3-axis accelerometer on the same silicon die, together with an onboard Digital Motion Processor™ (DMP™), which processes complex 6-axis Motion Fusion algorithms (Figure 15). The device can access external magnetometers or other sensors through an auxiliary master I²C bus, allowing the devices to gather a full set of sensor data without intervention from the system processor. It sense gravity from +/-1 to +/- 250. With three axes and up to 2000 DPS for X, Y and Z-axes. It communicates with microcontroller through I2C protocol (TDK Invense Sense, 2018).

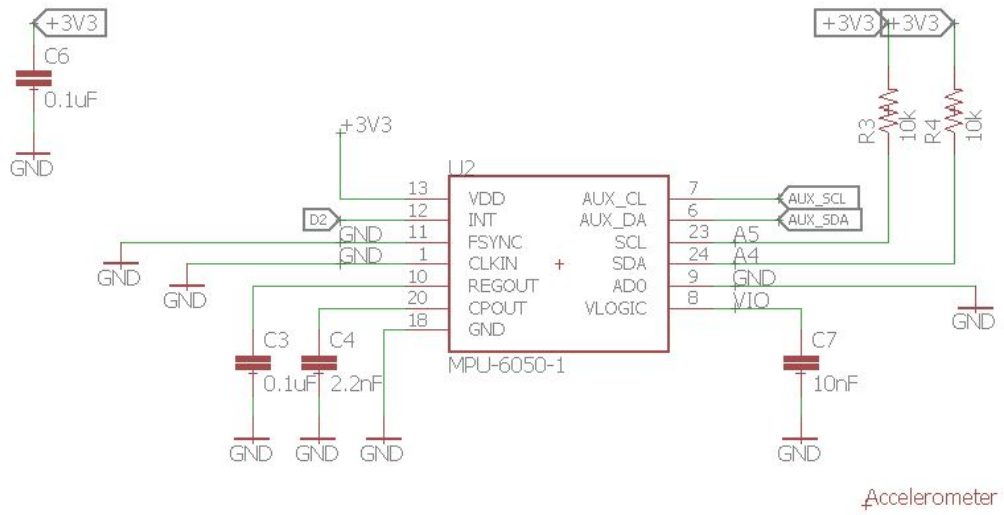

Figure 15. MPU 6050 circuit diagram.

Specifications of the MPU 6050

- Power supply: 3~5V onboard regulator
- Communication mode: Standard IIC communication protocol
- Chip built-in 16bit AD converter, 16bit data output
- Gyroscopes range: +/- 250 500 1000 2000 degree/sec
- Acceleration range: +/- 2g, +/- 4g, +/- 8g, +/- 16g
- Low pass filter response programmable range: 5-60 Hz
- Power spectral density @10Hz, 400 μg/√Hz

- Average current consumption 4 mA.

Heart Rate Sensor

The MAX30101 is an integrated pulse oximetry and heart rate monitor module (Figure 16). It includes internal LEDs, photo detectors, optical elements, and low-noise electronics with ambient light rejection. The MAX30101 provides a complete system solution to ease the design-in process for mobile and wearable devices (Maxim Integrated, 2016a).

The MAX30101 operates on a single 1.8V power supply and a separate 5.0V power supply for the internal LEDs. Communication is through a standard I^2C-compatible interface. The module can be shut down through software with zero standby current, allowing the power rails to remain powered always (Maxim Integrated, 2016a).

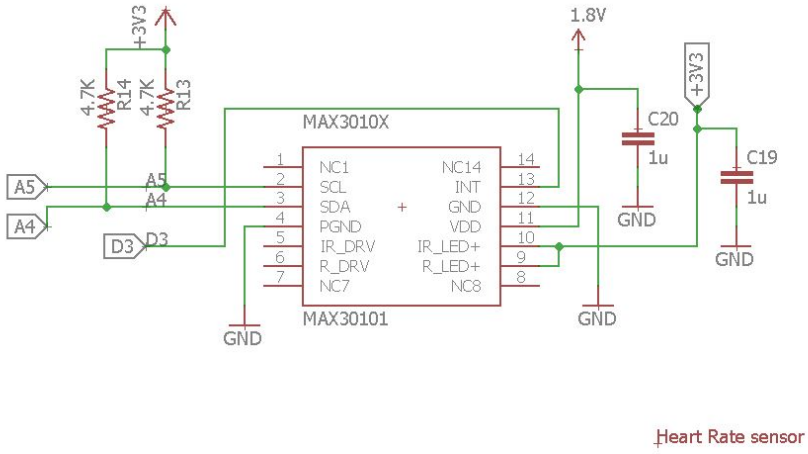

Figure 16. MAX30101 circuit diagram.

Specifications of the MAX30101

- Pulse oximetry or SpO2
- Programmable sample rate
- Interface: I2C,GPIO
- Input voltage: 3.3V or 5V
- Power consumption: <1mW
- -40°C to +85°C operating temperature range

- High SNR

Temperature Sensor

The MAX30205 temperature sensor accurately measures temperature and provides an over temperature alarm/interrupt/shutdown output (Figure 17). This device converts the temperature measurements to digital form using a high-resolution, sigma-delta analog-to-digital converter (ADC). Accuracy meets clinical thermometry specification of the ASTM E1112 when soldered on the final PCB. Communication is through an I^2C-compatible 2-wire serial interface (Nordic Semiconductor, 2016). The I^2C serial interface accepts standard write byte, read byte, send byte, and receive byte commands to read the temperature data and configure the behaviour of the open-drain over temperature shutdown output.

The MAX30205 features three address select lines, with a total of 32 available addresses. The sensor has a 2.7V to 3.3V supply voltage range, low 600µA supply current, and a lockup-protected I^2C-compatible interface that makes it ideal for wearable fitness and medical applications (Nordic Semiconductor, 2016).

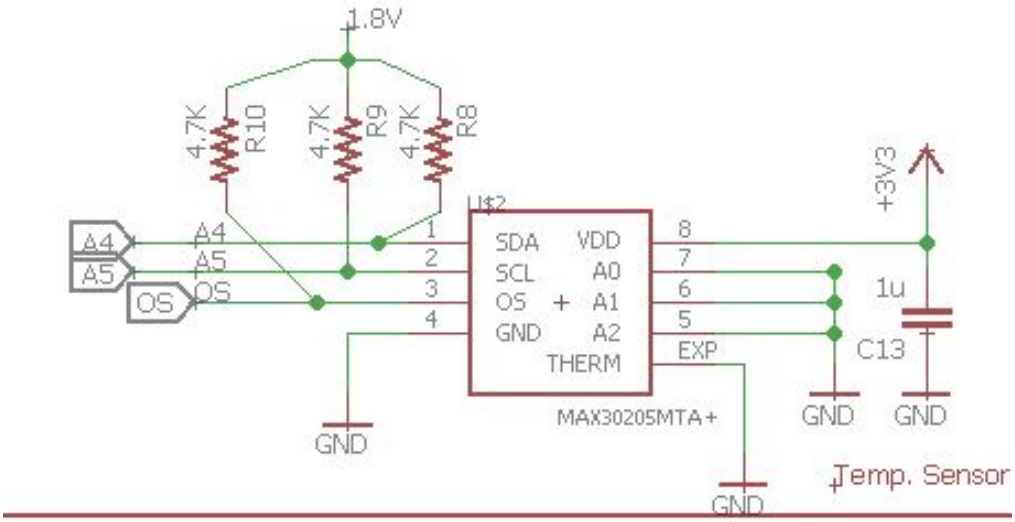

Figure 17. MAX3020 circuit diagram.

Specifications of the MAX3020

- 2.7V to 3.3V supply voltage range

- 16-bit temperature resolution
- 600uA operating supply current
- 0.1 degree/C accuracy (37 degree/C to 39 degree/C)

Wireless Module

The nRF24L01 is a highly integrated, ultra low power (ULP) 2Mbps RF transceiver IC for the 2.4GHz ISM (industrial, scientific and medical) band (Figure 18). With peak RX/TX currents lower than 14mA, a sub μA power down mode, advanced power management, and a 1.9 to 3.6V supply range, the nRF24L01 provides a true ULP solution enabling months to years of battery lifetime when running on coin cells or AA/AAA batteries (Texas Instruments, 2014).

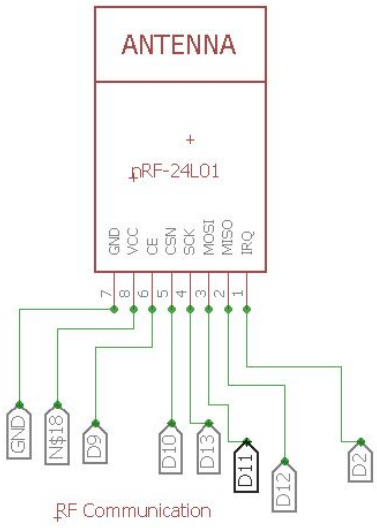

Figure 18. nRF 24L01 block diagram.

Specifications of the nRF24L01

- Worldwide 2.4GHz ISM band operation
- Up to 2Mbps on air data rate
- Ultra low power operation
- 11.3mA TX at 0dBm output power
- 12.3mA RX at 2Mbps air data rate

- 900nA in power down
- 22μA in standby-I
- On chip voltage regulator
- 1.9 to 3.6V supply range
- Enhanced ShockBurst™
- Automatic packet handling
- Auto packet transaction handling
- 6 data pipe MultiCeiver™
- Low cost BOM
- ±60ppm 16MHz crystal
- 5V tolerant inputs

Battery and USB Power Management Circuit

The Texas Instruments bq27441-G1 fuel gauge is a microcontroller peripheral that provides system-side battery fuel gauging based on patented fuel gauging for single-cell Li-Ion batteries (Figure19). The Impedance Track™ Technology device requires minimal user configuration and reports remaining capacity and state-of-system microcontroller firmware development (Texas Instruments, 2015).

The bq2407x series of devices are integrated Li-Ion linear chargers and system power path management devices targeted at space-limited portable applications. The devices operate from either a USB port or an AC adapter, and support charge currents up to 1.5 A. The input voltage range with input overvoltage protection supports unregulated adapters. The USB input current limit accuracy and start up sequence allow the bq2407x to meet USB-IF inrush current specifications. Additionally, the input dynamic power management (V_{IN}-DPM) prevents the charger from crashing incorrectly configured USB sources (SK Pang, n.d.).

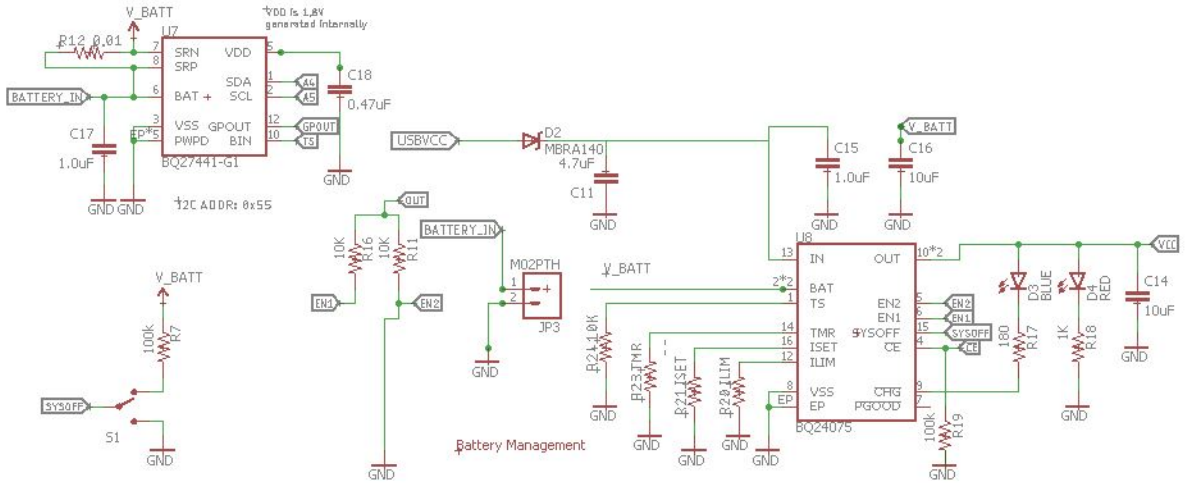

Figure 19. Power management circuit diagram.

Specifications of the Power Management Circuit

- Precision 16-bit, high-side coulomb counter with low-value sense resistor (5 mΩ to 20 mΩ)
- External and internal temperature sensors for battery temperature reporting
- Lifetime and current data logging
- 64 bytes of non-volatile scratch pad flash
- SHA-1 authentication capability
- Battery fuel gauging based on patented Impedance Track™ Technology
- Models battery discharge curve for accurate time-to-empty predictions
- Automatically adjusts for aging, self-discharge, and temperature: Rate induced effects on battery
- Integrated high-side NMOS protection FET drive
- Hardware-based safety and protection
- Overvoltage (OVP) – Undervoltage (UVP)
- Overcurrent in Charge (OCC) – Overcurrent in Discharge (OCD)
- Short-Circuit in Discharge (SCD)

- I 2C and HDQ interface formats for communication with host system
- Ultra-compact, 15-ball NanoFree™ DSBGA

Specifications of the BQ24075

- Number of series cells: 1
- Function: Charger
- Cell chemistry: Li-Ion/Li-polymer
- Battery charge voltage (min) (V): 4.2 V
- Battery charge voltage (max) (V): 4.2V
- Features: Power path

  Temp monitoring (thermistor pin)

  Vin DPM (OK for solar power source)
- Charge current (max) (A): 1.5 A
- Control interface: Standalone (RC-settable)
- Control topology: Linear.
- Operating temperature range (C) - -40 to 85
- Operating vin (min) (V): 4.2
- Operating vin (max) (V): 4.2

LCD 5110

The LCD 5110 (Figure 20) is a 48 x 84 Dot LCD Graphic that has the internal controller/driver "PCD8544" to control all displays and operations (allelectronic.com, 2012).

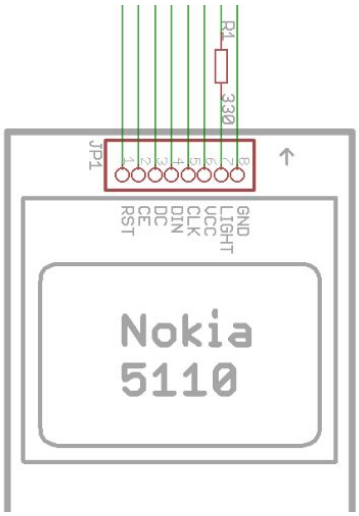

Figure 20. LCD display block diagram.

Specifications of the LCD 5110

- 48 x 84 dot LCD display *f*
- Serial bus interface with maximum high speed 4.0 Mbits/S *f*
- Internal Controller No.PCD8544 *f*
- LED back-light *f*
- Run at voltage 2.7 -5.0 Volt *f*
- Low power consumption;
- Suitable for battery applications *f*
- Temperature range from -25˚C to +70˚C
- Support signal CMOS

Audio Processor

The voice record module is based on the ISD1820, which is a multiple message record/playback device (Figure 21). It can offer true single chip voice recording, no volatile storage, and playback capability for 8 to 20 seconds. The sample is 3.2k and totals in the 20s for the recorder (Silicon Labs, 2018a).

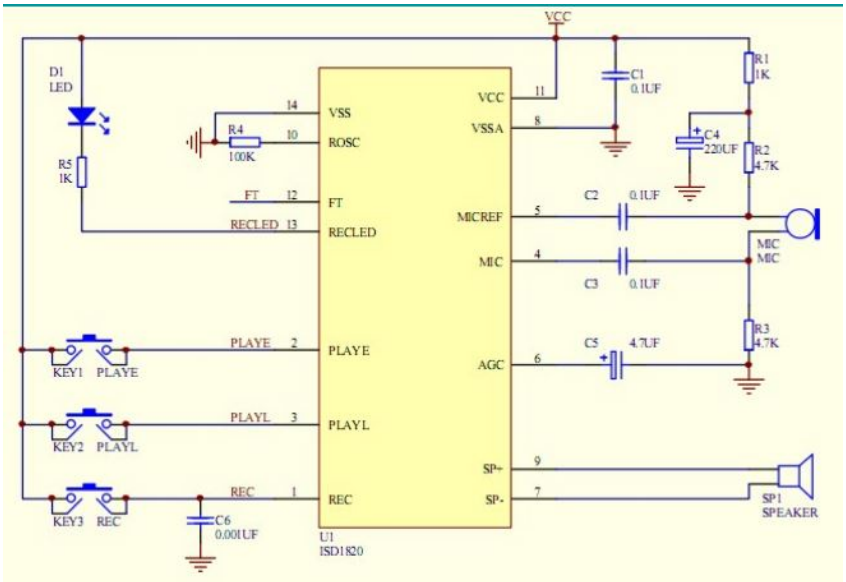

Figure 21. ISD 1820 circuit diagram.

Specifications of the ISD 1820

- Automatic power down mode
- Signal 3V power supply
- Sample rate and duration changeable by replacing a single resistor
- Record up to 20 seconds of audio

PCB layout of Wise Hand-I

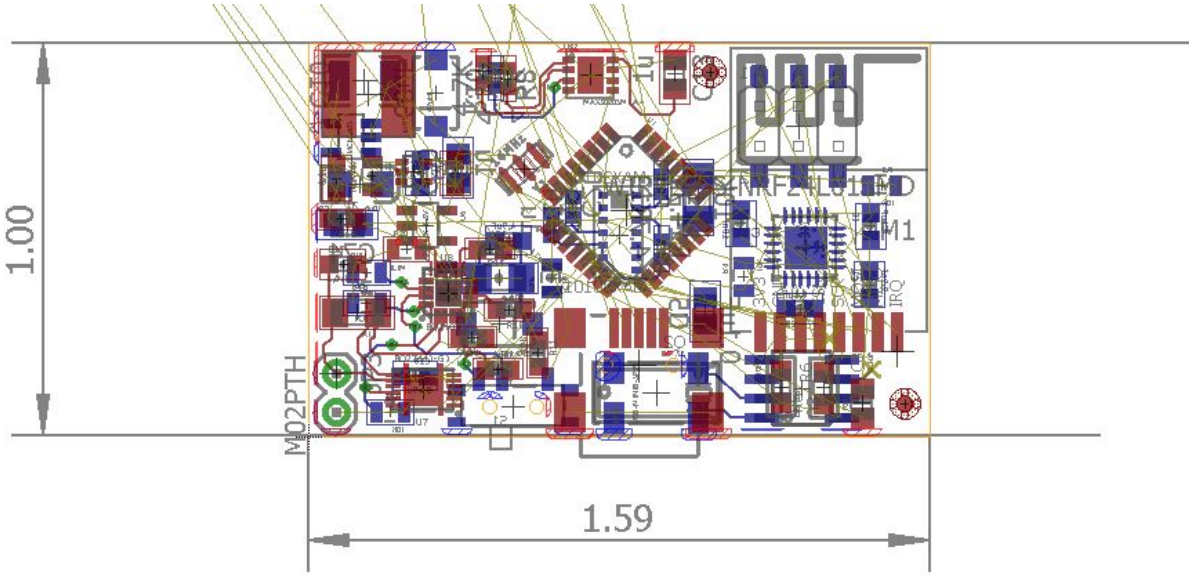

Figure 22. First prototype PCB design.

For PCB designing of Wise Hand –I, the Eagle CAD tool was utilized. Figure 22 shows the placement all components on both layers, top and bottom. As much as possible was optimized, but size of this PCB was not satisfactory in terms of wearable technology. The above figure shows the size of the PCB (1'' X 1.59").

Software for Wise-Hand-I

In the Wise Hand-I designed, there was no involvement of mobile apps, so only Arduino IDE software was used for programming the microcontroller. The following is an example code configuring the MPU6050 accelerometer register (Figure 23).

```
void setupMPU() {
  Wire.beginTransmission(0b1101000); //This is the I2C address of the MPU (b1101000/b1101001 for AC0 low/high datasheet sec. 9.2)
  Wire.write(0x6B); //Accessing the register 6B - Power Management (Sec. 4.28)
  Wire.write(0b00000000); //Setting SLEEP register to 0. (Required; see Note on p. 9)
  Wire.endTransmission();
  Wire.beginTransmission(0b1101000); //I2C address of the MPU
  Wire.write(0x1B); //Accessing the register 1B - Gyroscope Configuration (Sec. 4.4)
  Wire.write(0x00000000); //Setting the gyro to full scale +/- 250deg./s
  Wire.endTransmission();
  Wire.beginTransmission(0b1101000); //I2C address of the MPU
  Wire.write(0x1C); //Accessing the register 1C - Acccelerometer Configuration (Sec. 4.5)
  Wire.write(0b00000000); //Setting the accel to +/- 2g
  Wire.endTransmission();
}
```

```
void recordAccelRegisters() {
  Wire.beginTransmission(0b1101000); //I2C address of the MPU
  Wire.write(0x3B); //Starting register for Accel Readings
  Wire.endTransmission();
  Wire.requestFrom(0b1101000, 6); //Request Accel Registers (3B - 40)
  while (Wire.available() < 6);
  accelX = Wire.read() << 8 | Wire.read(); //Store first two bytes into accelX
  accelY = Wire.read() << 8 | Wire.read(); //Store middle two bytes into accelY
  accelZ = Wire.read() << 8 | Wire.read(); //Store last two bytes into accelZ
  gForceX = accelX / 16384.0;
  gForceY = accelY / 16384.0;
  gForceZ = accelZ / 16384.0;
}
```

```
void recordGyroRegisters() {
  Wire.beginTransmission(0b1101000); //I2C address of the MPU
  Wire.write(0x43); //Starting register for Gyro Readings
  Wire.endTransmission();
  Wire.requestFrom(0b1101000, 6); //Request Gyro Registers (43 - 48)
  while (Wire.available() < 6);
  gyroX = Wire.read() << 8 | Wire.read(); //Store first two bytes into accelX
  gyroY = Wire.read() << 8 | Wire.read(); //Store middle two bytes into accelY
  gyroZ = Wire.read() << 8 | Wire.read(); //Store last two bytes into accelZ
  rotX = gyroX / 131.0;
  rotY = gyroY / 131.0;
  rotZ = gyroZ / 131.0;
```

Figure 23. MPU 6050 configuration code.

Wise Hand-I Review

The Wise Hand-I contains total three hardware modules: (1) bracelet hardware, (2) configure/monitor module, and (3) audio module. The microcontroller used in Wise Hand-I is 8 bit controller that operates on 16 Mhz, and is capable of operating with a manual detection technique; however, with the automatic detection technique (i.e., FFT) there are some limitations with speed and resolution. Also, the PCB size of the bracelet i.e., module-I was not feasible for wearing nor for making a small bracelet. Furthermore, it was restricted to only hardware-to-hardware communication and not to Mobile Apps because wireless communication based on the nRFL01 is not compatible Bluetooth communication. The nRFL01 is not recommended for final product.

To overcome the issues in Wise Hand-I in terms of speed, resolution, accuracy, size and wireless communication, the first prototype was updated and named *Wise Hand-II.* Instead using a separate microcontroller and wireless module, a single SoC (System in Chip) was used; i.e., arm cortex and multi-protocols threads like BLE and ZigBee from Silicon Lab called EFR32, which is integrated with 32-bit arm cortex and Bluetooth and operates on a 32 MHz clock. Moreover, the wireless module used in Wise Hand-I is not low energy (i.e., power consumption was more compared to BLE). Another important update was mobile apps, as the first prototype design did not have mobile apps, which also sends data to a cloud database and allows easy access. For better accuracy and less noise data from accelerometer data, the MPU6050 was replaced with the ICM20468

Hardware Design of the Wise Hand-II

In the Wise-Hand-II, the microcontroller and nRfL01 was replaced with Single EFR32 Soc and Module-II with Mobiles Apps. For designing Wise-Hand-II, Altium CAD tools were used, and for simulation of sensor data, Matlab tools were used.

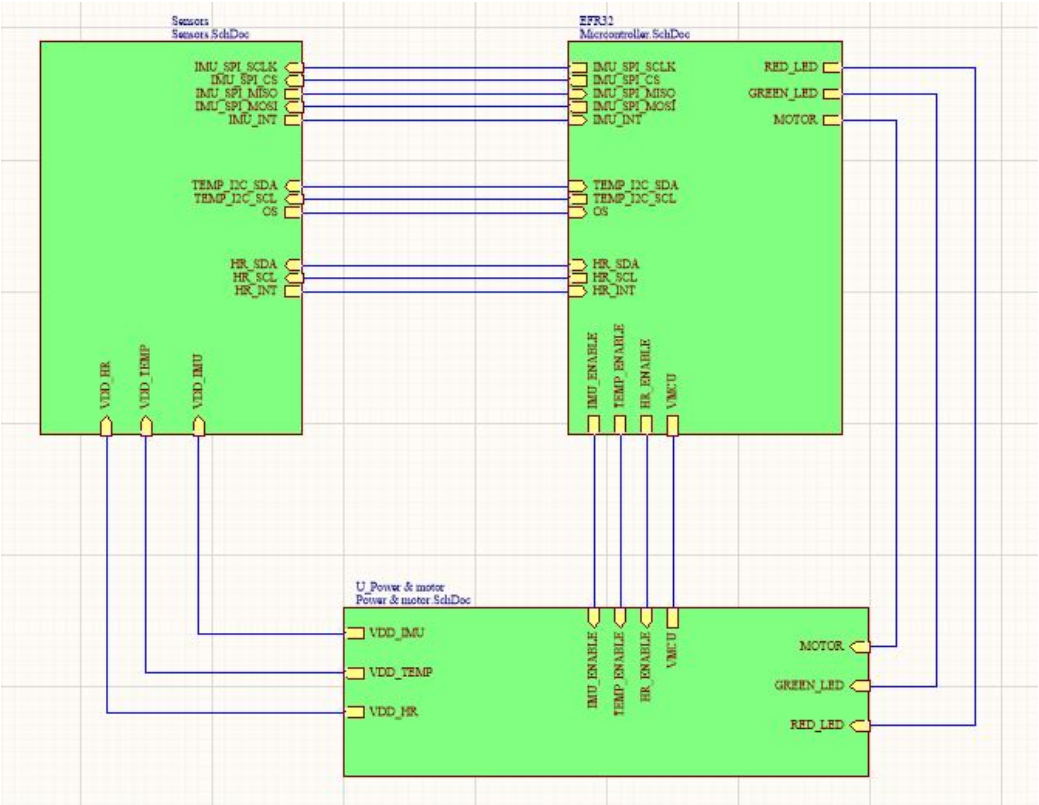

Figure 24. Smart bracelet schematic block diagram.

Microcontroller Design

The EFR32MG12P432F1024GL125 includes a 40 MHz ARM Cortex-M4 microcontroller with 1024 Flash, 256 RAM, and a richer peripheral set in a BGA125 package (Figure 25). With 19-dBm maximum power output and receiving sensitivity of -102.7 (250 kbps O-QPSK DSSS), the EFR32MG12P432F1024GL125 provides an excellent link budget for greater range and reliable RF communications. Built with low-power Gecko Technology, which includes innovative low energy techniques, fast wake-up times, and energy saving modes, the EFR32MG12P432F1024GL125 reduces overall power consumption and maximizes battery life. The EFR32MG12P432F1024GL125 includes wireless networking stacks for ZigBee and thread, and Bluetooth low energy. The device also includes support for proprietary wireless protocol development (Silicon Labs, 2018b).

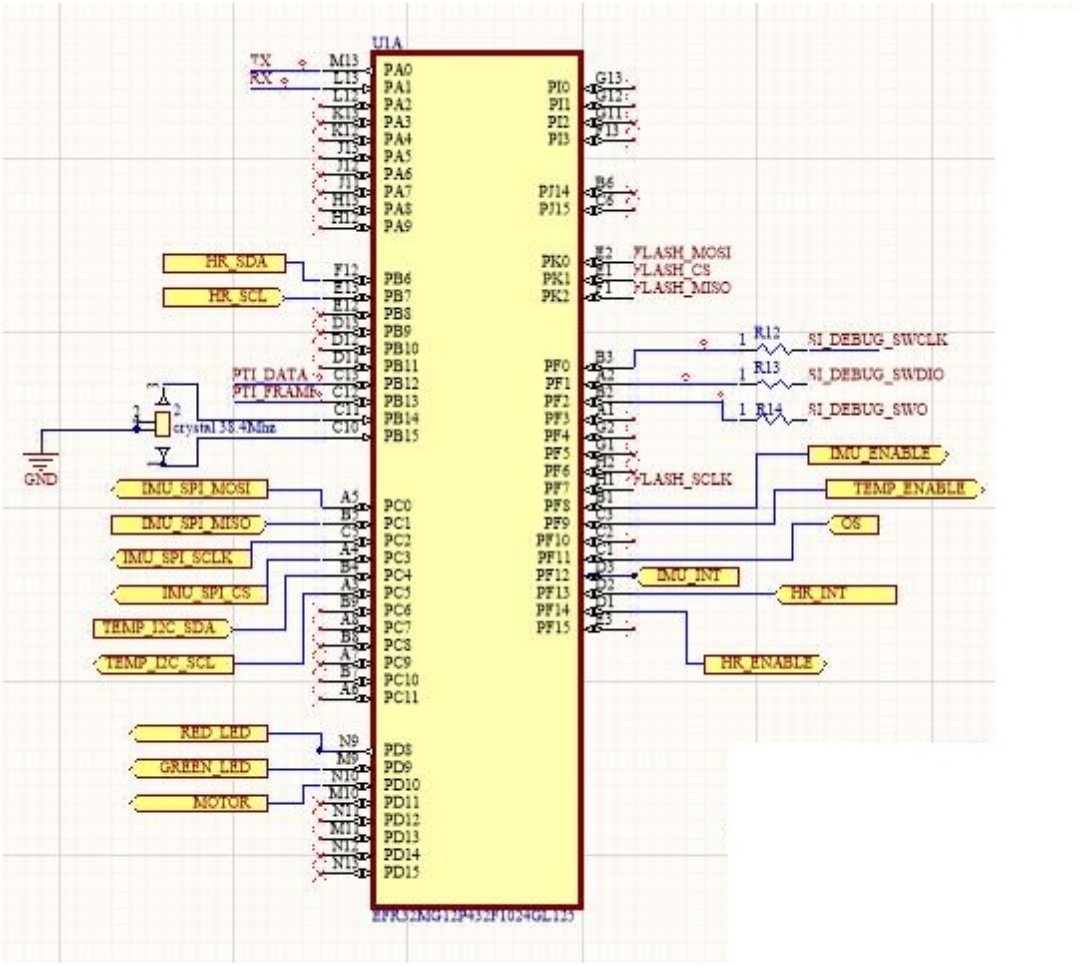

Figure 25. EFR32 part A circuit diagram.

Specifications of the EFR32 Part A

- 32-bit ARM® Cortex®-M4 core with 40 MHz maximum operating frequency
- Up to 1 MB of flash and 256 kB of RAM
- Pin-compatible across EFR32MG families (exceptions apply for 5V-tolerant pins)
- 12-channel peripheral reflex system, low-energy sensor interface and multichannel capacitive sense interface
- Autonomous hardware crypto accelerator and true random number generator
- Integrated PA with up to 19 dBm (2.4 GHz) or 20 dBm (Sub-GHz) TX power
- Integrated balun for 2.4 GHz

- Robust peripheral set and up to 65 GPIO

Wireless Communication Design

The EFR32 offers multi-protocols like ZigBee and BLE (Silicon Labs, 2018b). BLE protocols were utilized as the primary intention of wireless communication for mobile apps (Figure 26).

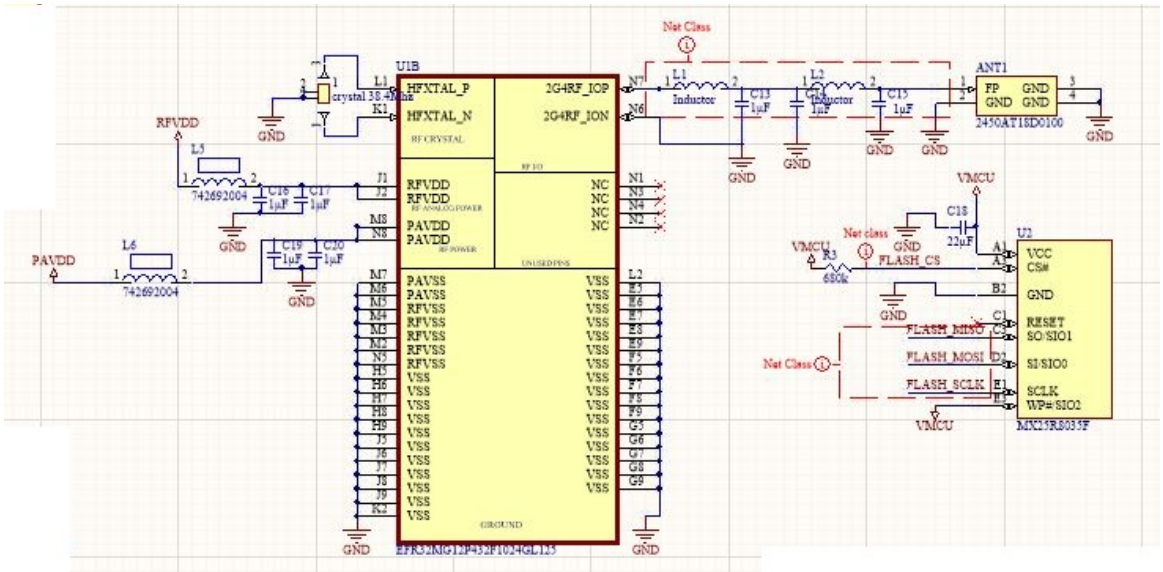

Figure 26. EFR32 part B circuit diagram.

Specifications of the EFR32 Part B

- ZigBee
- Thread
- Bluetooth® low energy (Bluetooth 5)
- Proprietary protocols
- Wireless M-Bus
- Selected IEEE 802.15.4g SUN-FSK PHYs
- Low power wide area networks
- Integrated PA with up to 19 dBm (2.4 GHz) or 20 dBm (Sub-GHz) TX power
- Integrated balun for 2.4 GHz

Power Section of Controller and BLE

The EFR32MG12 has an energy management unit (EMU) and efficient integrated regulators to generate internal supply voltages (Silicon Labs, 2018b). Only a single external supply voltage is required, from which all internal voltages are created. An optional integrated DC-DC buck regulator can be utilized to further reduce the current consumption. The DC-DC regulator requires one external inductor and one external capacitor. The EFR32MG12 device family includes support for internal supply voltage scaling, as well as two different power domains groups for peripherals. These enhancements allow for further supply current reductions and lower overall power consumption. AVDD and VREGVDD need to be 1.8 V or higher for the MCU to operate across all conditions; however the rest of the system will operate down to 1.62 V, including the digital supply and I/O. This means that the device is fully compatible with 1.8 V components. Running from a sufficiently high supply, the device can use the DC-DC to regulate voltage not only for itself, but also for other PCB components, supplying up to a total of 200 mA (Silicon Labs, 2018b).

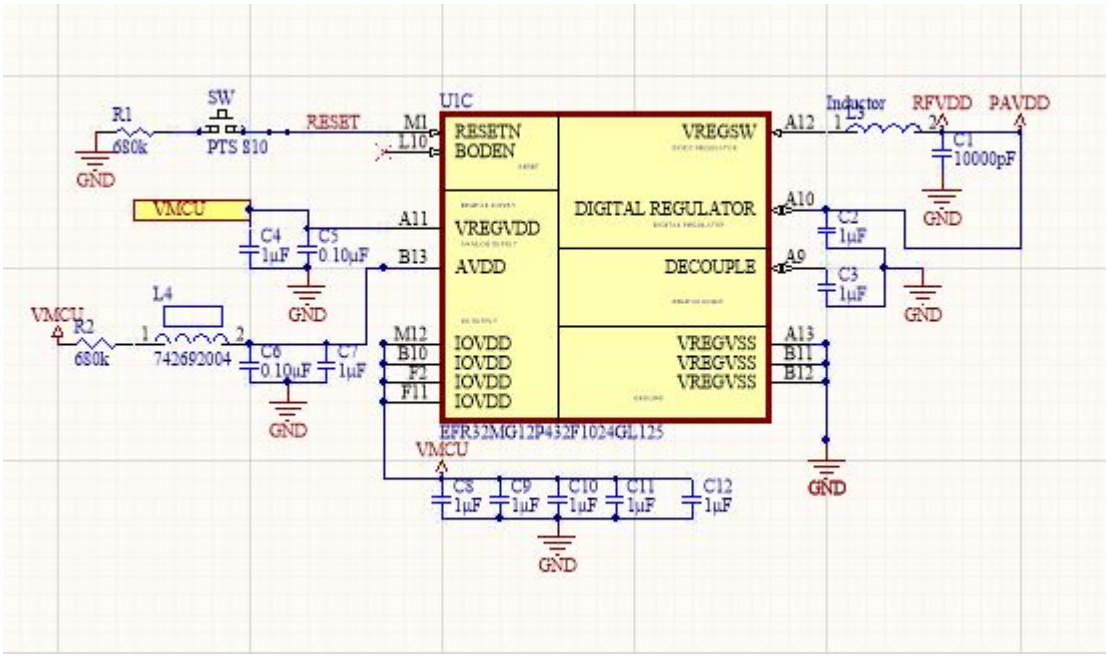

Figure 27. EFR32 part C circuit diagram.

ICM 20468 Design

As the MPU6050 was replaced with ICM20468 in the second design, the working and acceleration ranges of both sensors are same; the only difference tis hey have is noise performance and accuracy and electrical parameters (Figure 28).

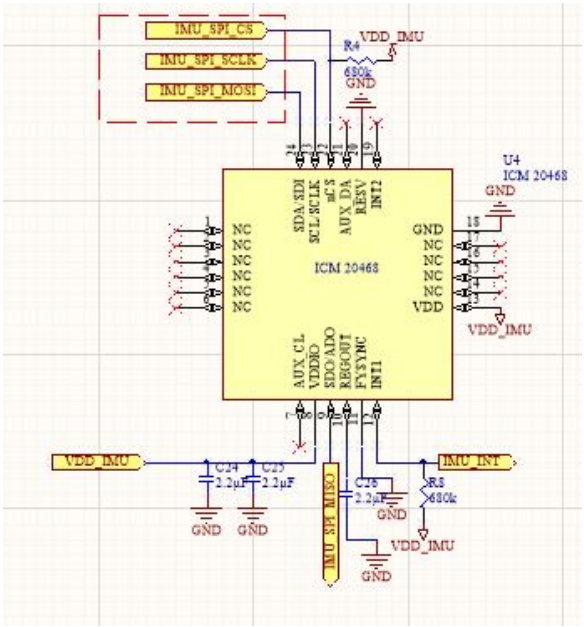

Figure 28. ICM 20468 circuit diagram.

Motor and LED Circuit Design

The vibration motor is again an important part of this system, as it enables the distraction for kids who have autism from hand flapping motion. Figures 29 and 30 show the circuit design for motor in system, which basically operates at 3.3V and the ON and OFF motor transistor being used as switch.

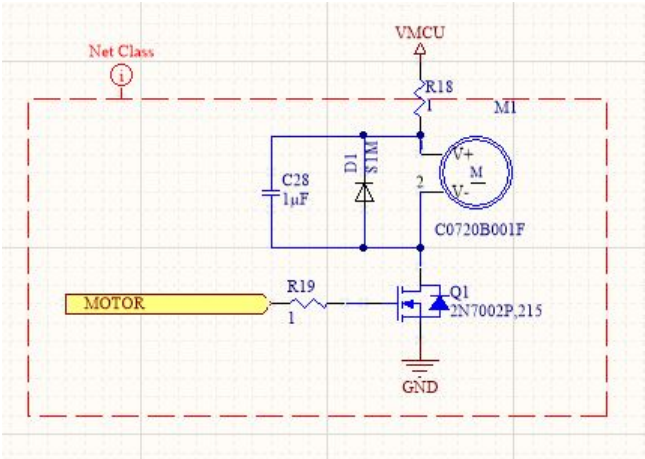

Figure 29. Motor activate circuit.

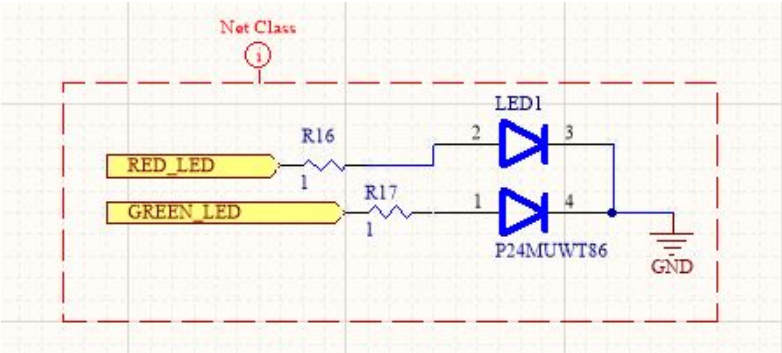

Figure 30. LED circuit.

Power Calculation

Power calculation is a main factor that must be considered very deeply, as this system is going to be categorized in wearable technology; that is, the system should be designed in such way that it will consume less energy. The following table shows power consumption by each section of system.

Table 4

Power Consumption Calculation

Part	Current (A)	Voltage (V)	Power (W)
EFR 32	200mA	3.3V	0.66 W
ICM 20468	500uA	3.3V	0.00165W
Heart Sensor	50mA	3.3V	0.165W
Temperature Sensor	40mA	3.3V	0.132W
Motor	20mA	3.3V	0.066W

Mobile Apps

The Wise Hand was updated with Mobile Apps to configure and monitor, as well cloud the data. Mobile Apps were designed in Android for showing proof of concept. Silicon Labs (2018b) resources were used to build Mobile Apps (Figure 31).

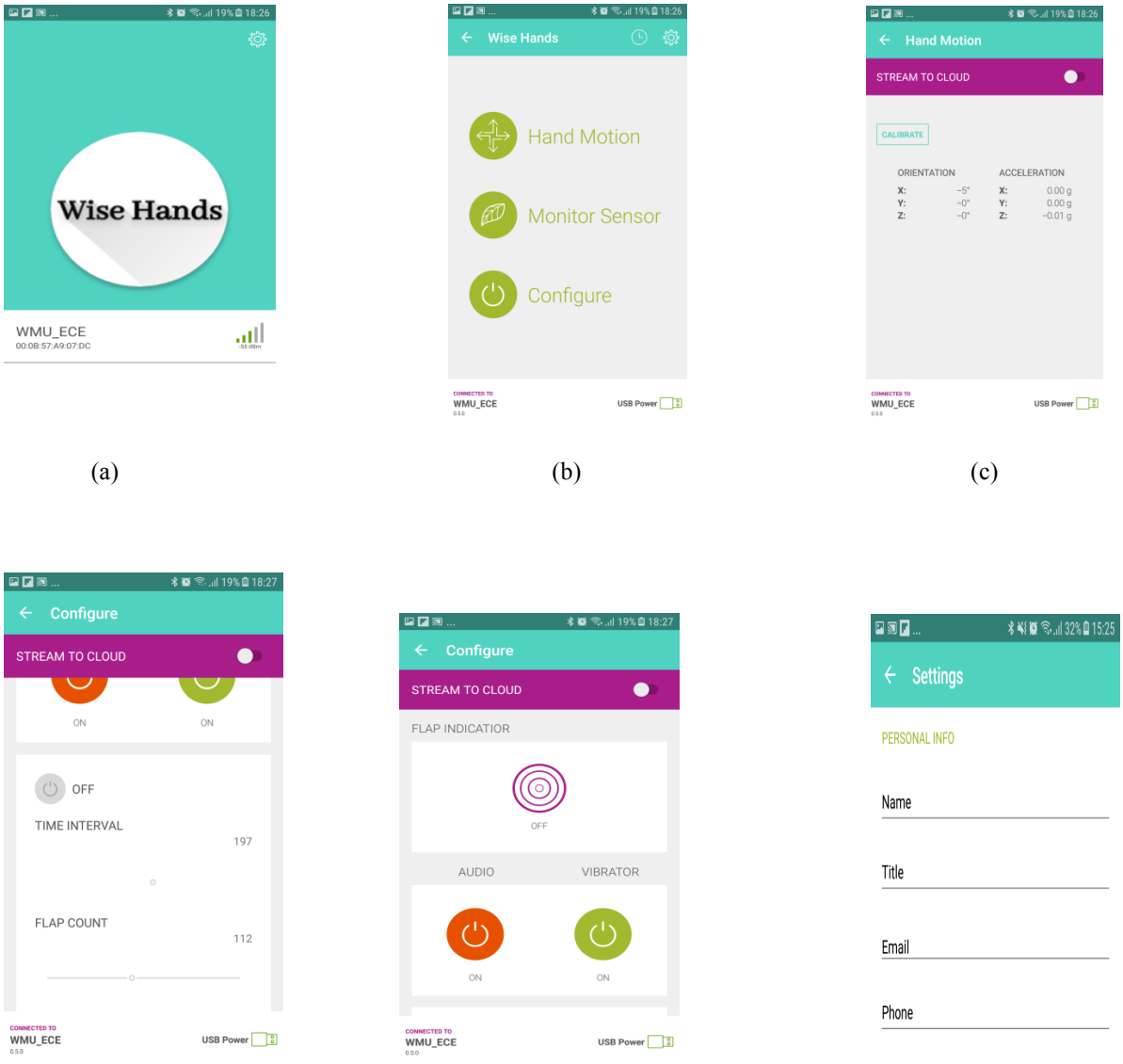

(a) (b) (c)

(d) (e) (f)

Figure 31. Mobile Apps screenshots.

Figure 31(a) shows an open page of Mobile Apps as it is searching for Bluetooth from the wrist band system with the name **WMU_ECE**. Once connection is established, it is directed to the home menu.

Figure 31(b) shows menu options of Wise Hand Apps, as it has three main options: (1) Hand Motion, (2) Monitor Sensor, and (3) Configure.

Figure 31(c) shows the monitoring accelerometer values along with calibration option through which the user can calibrate accelerometer values for more precise working.

Figure 31(d) shows the monitoring other sensor values. Now, it shows only temperature and humidity, but in the future it will have heart rate sensor as well.

Figure 31(e) is the configure menu, through which the user (i.e., parents and caretakers) can configure the wrist band module, such as setting threshold value for flap count, time interval, enable or disable motor and audio, along with flap indicator, which activates when uncertain behavior takes place.

Finally, Figure 31(f) shows, a feature on Mobile Apps where the user can fill out all of the information on the respective child, as this information is useful when the user clouds the sensor data online in a database, which saves the above information.

PCB Design

The Wise Hand-II is designed with Altium CAD tools, which are powerful compared to the Eagle tool used for designing first prototype. Wise Hand-II was designed with six layers of PCB. The first prototype PCB design had issues, as a small size design could not be achieved, but this was achieved in the Wise Hand-II design .

Hardware Requirements

Table 5 presents the component costs for the Wise Hand-II.

Table 5

Component Costs

Part	Quantity	Company	Cost
EFR32	1	Silicon Lab	$5
ICM20468	1	Inven sense	$3.50
MAX30101	1	Maxim Integrated	$5
MAX30205	1	Maxim Integrated	$2
Motor	1	Parallax	$3

Software for Wise Hand-II

In the Wise Hand-II design, the role of software occurred in two sections; one for writing firmware for the microcontroller, and the second for writing Java code for the mobile application used in Android studio.

For designing firmware for EFR32 i.e., the ARM controller and BLE, Simplicity Studio IDE was utilized, which is its own proprietary of Silicon Labs, and has function similar to IAR workbench. Simplicity Studio is proprietary IDE of Silicon Labs for debugging and compiling codes for their platforms.

To conclude, in Wise Hand-II, Mobile Apps was designed as a proof of concept for showing ease of feasibility. For writing code for Mobile Apps, Android Studio for writing Java code was utilized. The intention behind designing apps was to capitalize on the fact that everyone has a smart phone with internet connectivity, as well Bluetooth connection, which can help to connect to cloud and the smart bracelet respectively.

CHAPTER III

EXPERIMENTAL RESULT

The experimental results of this project are taken by simulating the hand flap motion in the laboratory, mimicking kids who have autism. To validate the results, three cases were considered that arise in the real-time scenarios in both the domains of time and frequency. To validate simulations result from both algorithms, data was taken from three different persons who had different styles of rest, walk, flap, and dance.

The following are simulation results from the first algorithm approached in Matlab in various actions like rest, walk, and flapping.

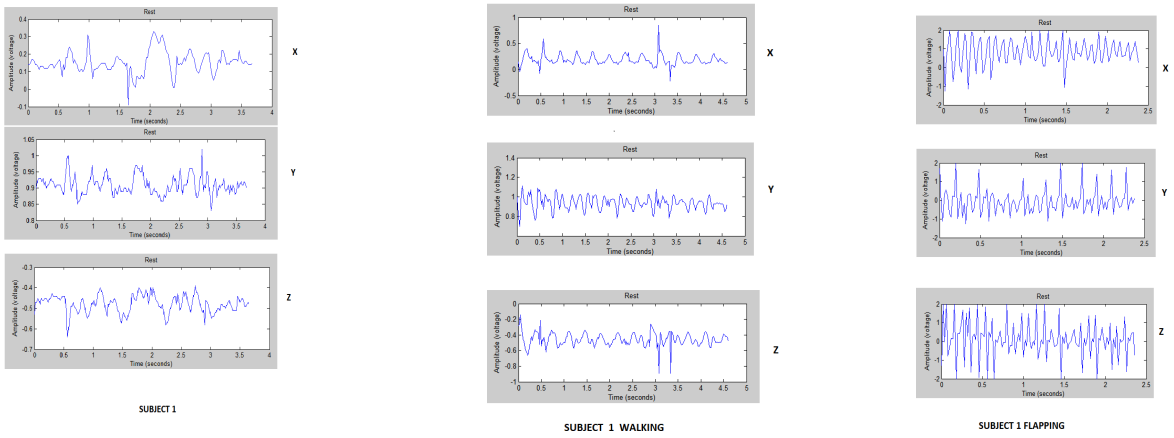

Figure 32. Rest, walk, and flapping time domain data.

Figure 32 shows the accelerometer data in three axes for approximately 4 seconds as subject was in rest position. Observations show that signals from X, Y, and Z were in the range of +0.5 to -0.5 acceleration. Similarly, in Figure 32 it was observed in walking action that there was same frequency data in range + 0.5 to -0.5 accelerations. Also, accelerometer data was simulated in flap action, so it was concluded in the first prototype design that acceleration values were high compared to rest and walk, and it was easy to classify this action in terms of rest, walk, and flap. Also, there was success in implementing the algorithm in microcontroller using language c and C++, in which code was looking for defined high

acceleration value within a defined time interval to identified as flap detection, which resulted into proper enabling of motor and sound.

The next challenge was to design a system with algorithms that were more reliable, more robust, and more accurate to achieve greater simulation results including getting more actions from different subjects. The following are simulation results in the Time domain from three different subjects in actions of rest, walk, flap and dance.

Case I: Rest in the Time Domain

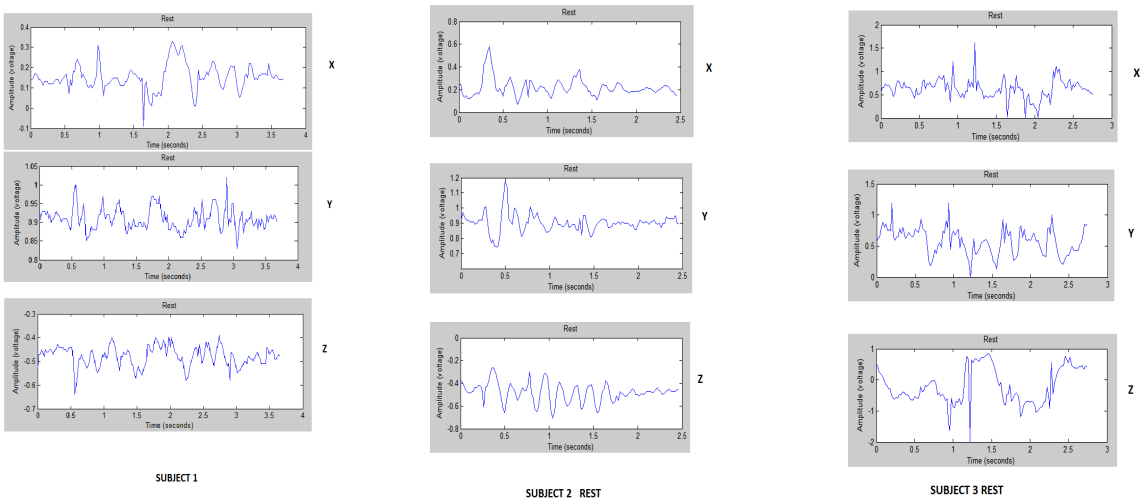

Figure 33. Rest data in time domain from three subjects.

It was observed that data was in almost same range for all three subjects.

Case II: Walking in the Time Domain

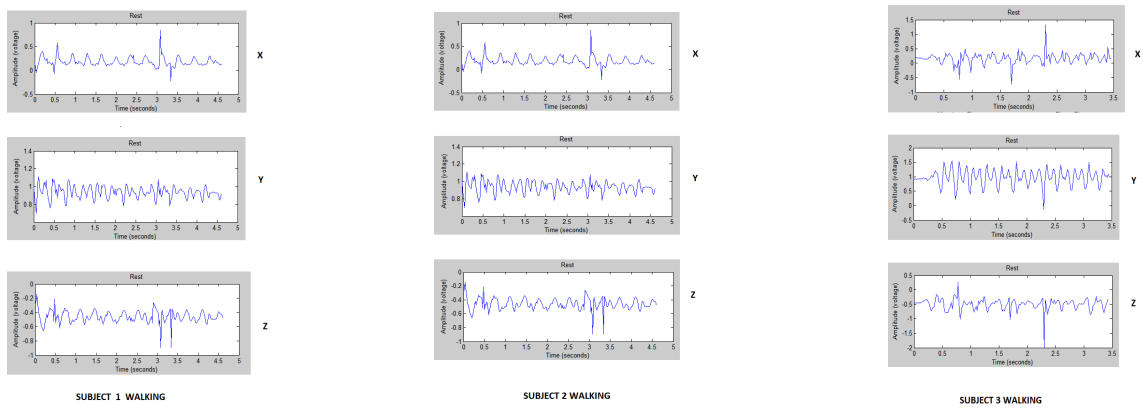

Figure 34. Walking data in time domain from three subjects.

Figure 34 shows data from Subjects 1, 2, and 3 respectively in walk action, and it was concluded that it was different from flap action.

Case III: Flapping in Time Domain

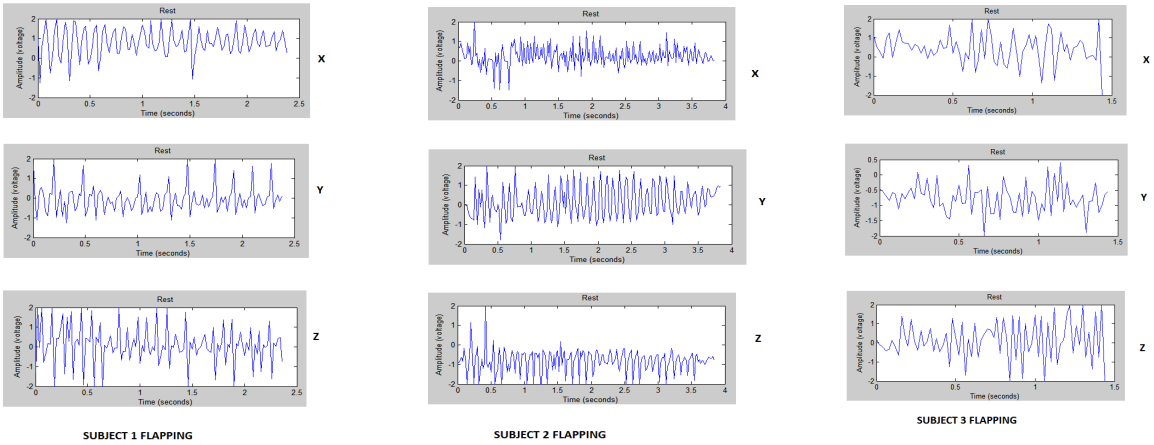

Figure 35. Flapping data in time domain from three subjects.

Data was also taken from three different subjects in flapping motion. Figure 35 shows these graphs and it was observed that flapping usually occurs in above range +1.5, with high frequency. It was also observed from Subject 3 that high acceleration data occurred, but more than the defined time interval.

Case IV: Dancing in Time Domain

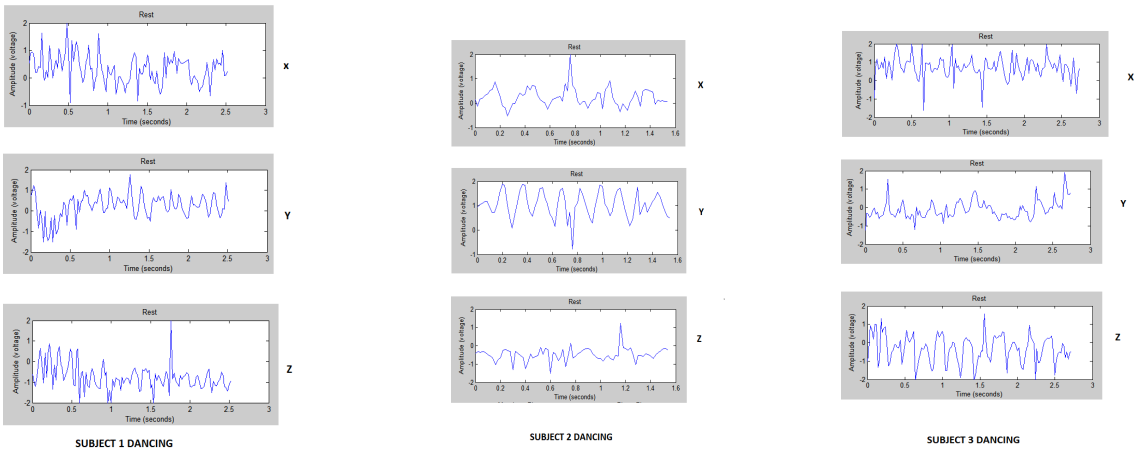

Figure 36. Dancing data in time domain from three subjects.

Also, while simulating dance action data from three different subjects, there was confused data observation, as some parts of dance data matched with flap action, which created issues in classifying dance and flap action. Figure 36 shows three axis graphs in dance action mode.

It was concluded that the Detection algorithm in the Time domain had some issues classifying hand motion. To make an improvement the research approached a second detection algorithm with the Frequency domain.

The following are simulation results from the Frequency domain classification.

Case I: Rest in Frequency Domain

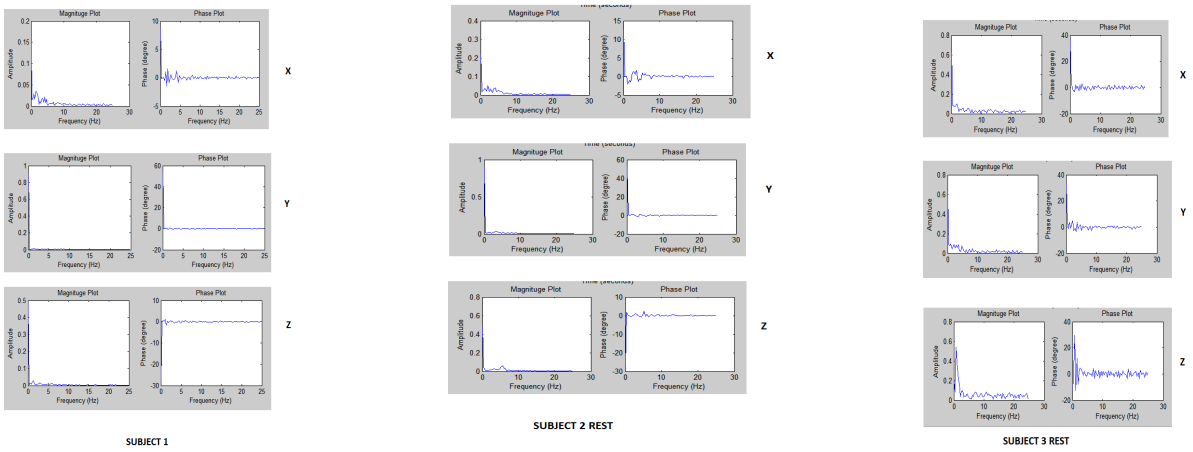

Figure 37. Rest data in frequency domain from three subjects.

Figure 37 shows the accelerometer data from Subject 1, 2, and 3 respectively in rest motion. Only occurred negligible amplitude frequency on X- axis data.

Case II: Walking in Frequency Domain

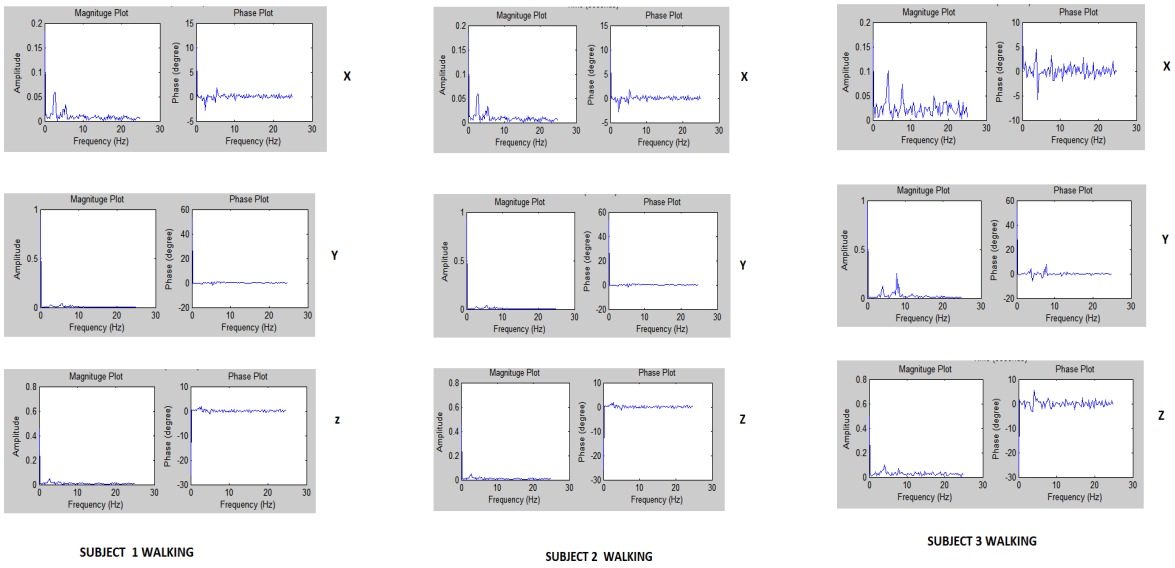

Figure 38. Walking data in frequency domain from three subjects.

Figure 38 shows that walking motion in three axis is not overlapping with flap motion.

Case III: Flapping in Frequency Domain

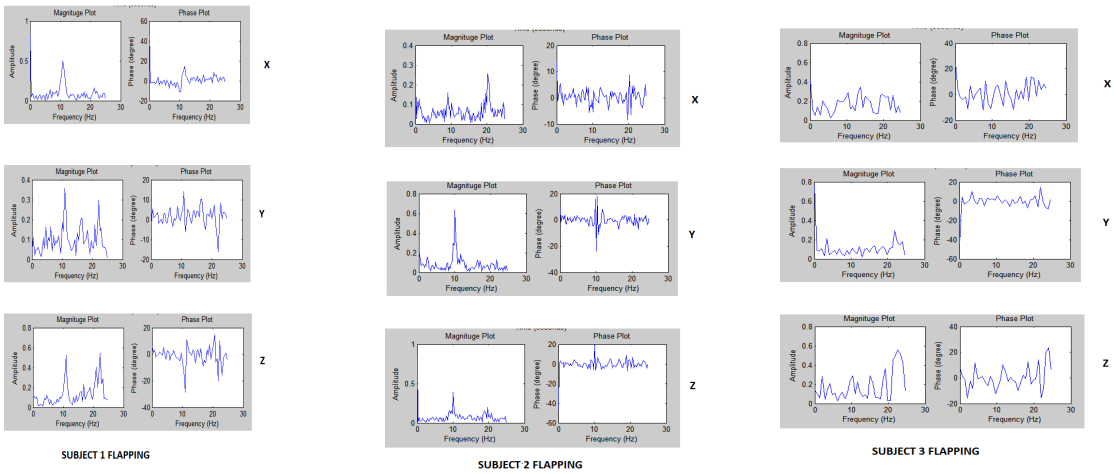

Figure 39. Flapping data in frequency domain from three subjects.

It is clearly observed that while simulating three axis data in flap motion, three was a window from approximately 8 Hz to 13 Hz with a magnitude around 0.5 that occurred in all three subjects flap motion. Figure 39 shows the Frequency domain graph for flap motion.

Case IV: Dancing in Frequency Domain

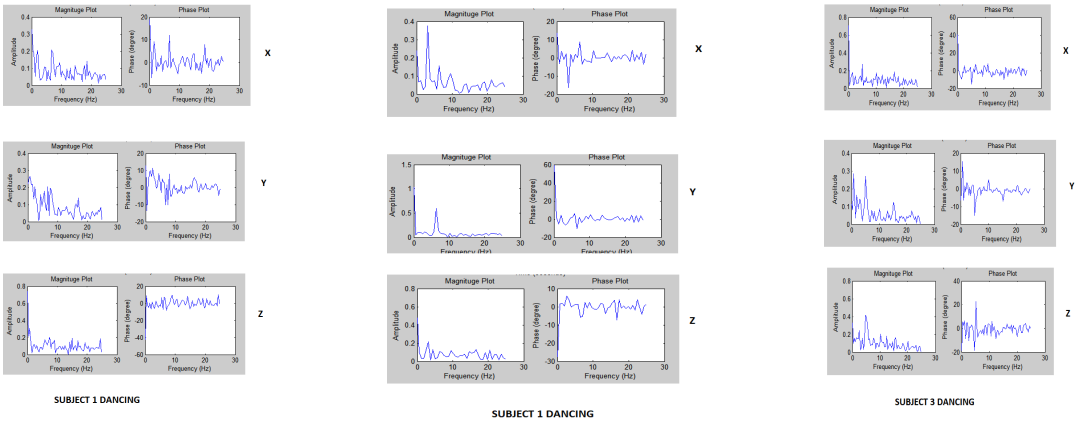

Figure 40. Dancing data in frequency domain from three subjects.

Finally, three axis data in dance motion was simulated, and it was observed that frequencies in dance motion did not overlap with flap motion. Thus, it was concluded that the detection algorithm in the Frequency domain is more accurate and efficient compare to the Time domain. Hence, with consideration of the Frequency domain detection, there was a change in hardware design to meet the Frequency domain requirements, as it requires a high speed processor and resulted into designing of Wise Hand-II, in which the ARM Cortex 32Bot microcontroller with Clock frequency 33 was used.

CHAPTER IV

CONCLUSION AND FUTURE SCOPE

In conclusion, this research project successfully addressed the problem of stereotypic and repetitive hand flapping motion in autistic children. The results and the plots indicate that the motor and audio device is triggered when the significant hand flap motion is detected. By varying the design parameters i.e., the predefined threshold value and the time span, the system can be customized to almost all of the hand flapping symptoms, depending on the severity of the disease. In addition, it can also be successfully used to detect the body rocking symptoms exhibited by the child.

By using the system regularly, the reminder system can have a very good impact on the behavior of the child over the course of time. The system can help in the overall behavior of the children and improve social acceptability. This also helps in preventing the child's behavior from turning into a self-injurious behavior. The learning ability of the children also increases gradually. The children need not be kept under the strict monitoring of parents and caregivers, as the system itself can remind the children of their stereotypic movement. It greatly reduces the burden of parents and caregivers.

With the advent of technology, all most all problems can be addressed successfully. We hope that this system brings a positive change in the lives of autistic children and their parents. However, no technology can ever compensate for human relations, especially for the children affected with autism. Good parenting always plays an essential role in the upbringing of children.

The reliability of the system can be improved by implementing machine learning techniques on the accelerometer and gyroscope data.

REFERENCES

Albinali, F., Goodwin, M. S., & Intille, S. S. (2009). Recognizing stereotypical motor movements in the laboratory and classroom: a case study with children on the autism spectrum. In Proceedings of the 11th International Conference on Ubiquitous Computing. Orlando, FL 71-80.

Allelectronic.com. (2012, October). ISD1820 Voice Recorder Module User Guide. Retrieved from https://www.allelectronics.com/mas_assets/theme/allelectronics/spec/ME-63.pdf

Autism Society. (2015, July 15). Causes. Retrieved from http://www.autism-society.org/what-is/causes/

Centers for Disease Control and Prevention. (2018, April 26). Autism Spectrum Disorder (ASD): Data & Statistics. Retrieved from https://www.cdc.gov/ncbddd/autism/data.html

Gonçalves, N., Rodrigues, J. L., Costa, S., & Soares, F. (2012c). Preliminary study on determining stereotypical motor movements. In Engineering in Medicine and Biology Society (EMBC), 2012 Annual International Conference of the IEEE. San Diego, CA. 1598-1601.

Maxim Integrated. (2016a). MAX30101. Retrieved from https://datasheets.maximintegrated.com/en/ds/MAX30101.pdf

Maxim Integrated. (2016b). MAX30205. Retrieved from https://www.maximintegrated.com/en/products/sensors-and-sensor-interface/MAX30205.html

Micrcochip. (2016, December 16). Atmega328. Retrieved from https://www.microchip.com/wwwproducts/en/ATmega328

Min, C.-H., & Tewfik, A. H. (2010). Automatic characterization and detection of behavioral patterns using linear predictive coding of accelerometer sensor data in Engineering in Medicine and Biology Society (EMBC). Paper presented at the International Conference of the IEEE.

Min, C.-H., Tewfik, A. H., Kim, Y., & Menard, R. (2009). Optimal sensor location for body sensor network to detect self-stimulatory behaviors of children with autism spectrum disorder. In Engineering in Medicine and Biology Society, 2009, Annual International Conference of the IEEE. Minneapolis, MN. 3489-3492.

Nordic Semiconductor. (2016). nRF24L01. Retrieved from http://www.nordicsemi.com/eng/Products/2.4GHz-RF/nRF24L01

Silicon Labs. (2018a). EFR32MG12P432F1024GL125 Zigbee and Thread Multiprotocol Mighty Gecko SoC. Retrieved from https://www.silabs.com/products/wireless/mesh-networking/efr32mg-Mighty-gecko-zigbee-thread-soc/device.efr32mg12p432f1024gl125

Silicon Labs. (2018b). Thunderboard™ Sense 2 Sensor-to-Cloud Advanced IoT Development Kit. Retrieved from https://www.silabs.com/products/development-tools/thunderboard/thunderboard-sense-two-kit

SK Pang. (n.d.). User's Manual of Graphic LCD "ET-NOKIA LCD 5110". Retrieved from http://skpang.co.uk/catalog/images/lcd/graphic/docs/User_Manual_ET_LCD5110.pdf

Sprague, R. L., & Newell, K. M. E. (1996). *Stereotyped movements: Brain and behavior relationships.* Washington, DC: American Psychological Association.

TDK Invense Sense. (2018). MPU-6050. Retrieved from https://www.invensense.com/products/motion-tracking/6-axis/mpu-6050/

Texas Instruments. (2014, December). bq27441-gl. Retrieved from http://www.ti.com/lit/ds/symlink/bq27441-g1.pdf

Texas Instruments. (2015, March). bq2407. Retrieved from http://www.ti.com/lit/ds/symlink/bq24075.pdf

Westeyn, T. Vadas, K., Bian, X., Starner, T., & Abowd, G. (2005). Recognizing mimicked autistic self-stimulatory behaviors using HMMs. Proceedings of the 2005 9th IEEE International Symposium on Wearable Computers.

Witten, I. & Frank, I.H. (2002). Data mining: Practical machine learning tools and techniques with JAVA implementations. Retrieved from ftp://ftp.ingv.it/pub/manuela.sbarra/Data%20Mining%20Practical%20Machine%20Learning%20Tools%20and%20Techniques%20-%20WEKA.pdf

Appendix A

Matlab Code

Matlab Code

```
clc;
clear all;
close all;


x = importdata('S2_Z_walk.txt');
T=1/50;
L=length(x);
Fs=1/T;
t=(0:L-1)*T;
Y = fft(x);
mag1 = abs(Y/L);
mag = mag1(1:L/2+1);
mag(2:end-1) = 2*mag(2:end-1);
ph1 = rad2deg(Y/L);
ph = ph1(1:L/2+1);
ph(2:end-1) = 2*ph(2:end-1);
f=Fs*(0:(L/2))/L;

%PLOTTING RESULTS
%--------------------------------------

subplot(2,2,[1,2])
plot(t,x);
title('Walk');
xlabel('Time (seconds)');
ylabel('Amplitude (voltage)');

subplot(2,2,3)
plot(f,mag);
title('Magnituge Plot');
xlabel('Frequency (Hz)');
ylabel('Amplitude');

subplot(2,2,4)
plot(f,ph);
title('Phase Plot');
xlabel('Frequency (Hz)');
ylabel('Phase (degree)');
```